Investigations into self motion thresholds using a Stewart platform

INVESTIGATIONS INTO SELF MOTION THRESHOLDS USING A STEWART PLATFORM

BY

BEHZAD AKBARI

AKBARIB@MCMASTER.CA, M.Sc.

A THESIS

SUBMITTED TO THE DEPARTMENT OF COMPUTER SCIENCE

AND THE SCHOOL OF GRADUATE STUDIES

OF MCMASTER UNIVERSITY

IN PARTIAL FULFILMENT OF THE REQUIREMENTS

FOR THE DEGREE OF

MASTER OF APPLIED SCIENCE

Master of Applied Science (2014) McMaster University

(Computer Science) Hamilton, Ontario, Canada

TITLE:	Investigations into self motion thresholds using a Stewart platform
AUTHOR:	Behzad Akbari akbarib@mcmaster.ca M.Sc., (Software Engineering) University, City, Country
SUPERVISOR:	Dr. Martin v. Mohrenschildt
NUMBER OF PAGES:	xi, 76

It is dedicated to my family, for devotion and endless support.

Acknowledgements

Foremost, I would like to express my sincere gratitude to my supervisor Dr. Martin Mohrenschildt for the continuous support of my research, for his patience, motivation, enthusiasm, and immense knowledge.

I would also like to thank you Miss Apurva Kumar for her worthwhile help in revising my thesis and Dr. John Grundy from the Psychology department who assisted in preparation for this paper.

Contents

List of Figures

Abstract

Full motion simulators are traditionally used in the flight industry to train pilots. They are used to add the sensation of acceleration in simulation to make it more "realistic". Clearly the motion envelop of the simulator is limited by physical constraints so the motion platform has to be stopped and returned to the center position after an acceleration cue, called washout. A key question is: which acceleration can a subject feel and which not and what is the acceleration threshold? We are also interested in strength of accelerations for which a subject can detect the direction. The literature gives several results, but some of these values seemed very low and the experiments were conducted on very specific groups of people like pilots, A.J.Benson and H.Vogel (1986), Schroeder (1999). Furthermore, we are simulating moving vehicles like a car or an air plane and are interested in the acceleration ranges in a noisy environment. The noise is a result from the vibration of engines, rough roads and disturbances , and are modelled as Gaussian.

This thesis gives a literature review, implements the cueing procedure to make motion and vibration to perform different experiments and analyzes the results.

Chapter 1

Introduction

The study of the human vestibular system is a recent development as in ancient times it was hidden within the ear. In fact, equilibrium was not even mentioned by Aristotle in his description of the five senses (sight, hearing, smell, taste and touch), Barnett-Cowan (2013). Today there are many fields that scholars are studying about the perception of whole-body stimuli, for example, psychophysics, medicine, aerospace, computer simulation and so on. Most of these studies investigate the characteristics of the vestibular sensory system which is now known as the sixth sense, Jay M. Goldberg (2012). In order to fully explain and simulate the physical phenomena which happen in this organ, a multi-disciplinary approach is required. Scientists in psychophysics, mechanics and computer science need to collaborate to derive accurate results. Many aspects of this organ are still unknown, like the effect of training or threshold bias in a noisy environment.

This thesis gives a literature review, implements the motion cueing algorithm on a hexapod motion simulator to produce linear acceleration and vibration, examines a number of experiments to compute the effects of training on accuracy of detection

and threshold bias in a noisy environment.

Creating the sensation of movement within the motion simulator (Motion Cueing) is a complicated task because the motion hardware displacements are subject to limitations. Vehicle movement can not be sent directly to the motion simulator therefore we need motion cueing strategies and washout algorithms. In fact motion cueing algorithms are required to translate the vehicle motion into valid simulator displacement.

To find vestibular system characteristics, one approach is to use motion cueing algorithms based on filtering. However, because of the difficulty in implementation and finding the accurate cut-of parameters, this project did not implement the full range of cueing algorithms. Instead, we developed a particular cueing algorithm to generate motion with a constant acceleration for a fixed duration. Then we washed out the simulator before passing the displacement limitations (Chapter 5). To mask mechanical auditory cues we used white noise during the experiment. We also installed two different accelerometers, AC and DC-response, to increase accuracy and not lose any information.

Our program was written using C++ under Linux to generate constant linear accelerations, implement the washout algorithm, and simulate vibrations for each trial. We used constant stimuli in which the levels of stimulus are presented randomly and are not related from one trial to the next. Our accelerations are between $0.01 \sim 0.2\frac{m}{s^2}$ with a washout acceleration under the threshold (e.g. $0.01\frac{m}{s^2}$) and we used this range of different accelerations randomly for each participant. This method was intended to prevent the participants from predicting the level of the next stimulus, therefore reducing habituation error, Gescheider (1997).

To compute accuracy and vestibular bias for each experiment, participants sat inside the platform and were asked to indicate on a keypad the direction of their motion. The software recorded their responses in real-time. We found the accuracy and response time for four participants who each completed four sessions, with four blocks in each section for a total of 168 trials per block. We computed learning effects across the four sessions. Our results indicate that participants could reliably discriminate motion direction for our acceleration profile (Table 6.3) within a noisy environment. Furthermore, their accuracy improved over time, resulting in decreased thresholds across sessions. Moreover, for forward movement we computed the proportion of answers (correct and incorrect) and we found a negative vestibular bias (Chapter 6).

The thesis is divided into two parts, in part I, (Background) we described vestibular system concepts and regular cueing algorithms and in part II (Method and Findings) we develop our design and provide results of our data analysis.

Part I

Background

Chapter 2

Vestibular system

2.1 Introduction

The vestibular system is the sensory mechanism of the inner ear (labyrinth) that detects motion of the head and makes reflexes that are crucial to our daily activities such as stabilizing the visual axis (gaze) and maintaining equilibrium, Kathleen Cullen (2008). Driving a car or plane, walking down a road, even maintaining balance, these are tasks that rely upon the continuous detection and integration of self-motion information.

The perception of linear motion has been less extensively studied than the perception of angular movements. This disparity is due to the greater difficulty of creating whole-body linear motion stimuli without existing mechanical and acoustical cues, Benson and Stott (1986).

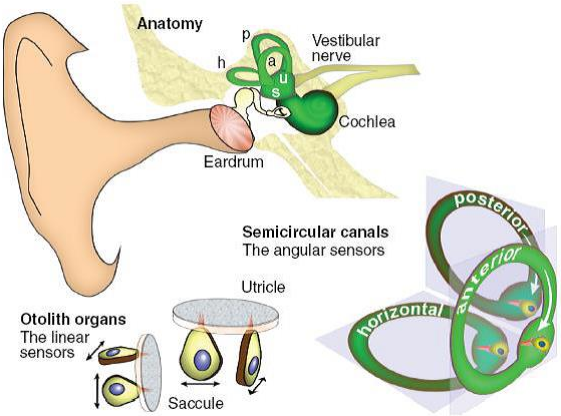

Figure 2.1: Vestibular system, Day and Fitzpatrick (2005)

2.1.1 Otolith organs and semicircular canals

Otolith organs and semicircular canals are two distinct sets of end organs in the labyrinth. The otolith organs (utricle and saccule) which respond to direction and magnitude of linear accelerations are stimulated in the position of the head with respect to gravity. Three semicircular canals respond to angular acceleration and rotational movements in three planes, Kathleen Cullen (2008).

The receptor cells of the otoliths and semicircular canals send signals through the vestibular nerve fibers to the neural structures that control eye movements, posture, and balance. The rotation of the head moves the endolymph inside the semicircular canals, causing a deflection of the cupula which excites the hairs and sensory cells. Depending on the excitation, information regarding sensed rotations is sent to the brain, Kathleen Cullen (2008).

According to Telban and Cardullo (2005) there are two otolith organs in the human ear, the utricle which senses horizontal motion and the saccule which senses

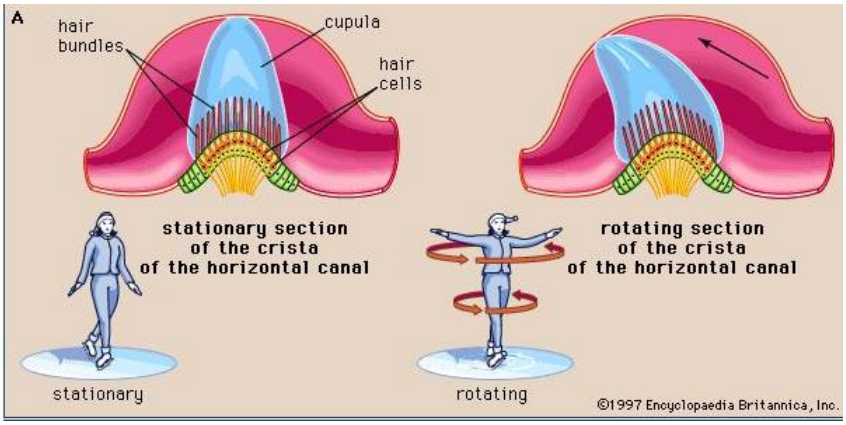

Figure 2.2: The receptor cells of the semicircular canal Britannica (2009)

vertical motion. Kathleen and Soroush believe the utricle and saccule are sensitive to direction and magnitude of linear acceleration.

As you can see in Figure 2.2, the translational movements of the head cause deflection of the otolithic membrane. This excites the sensory cells, and sends information about applied specific forces to the brain. Moreover the vestibular system is integrated with visual, proprioceptive and other sensory organs that lead to a sense of motion.

The vestibular system also plays a critical role in ensuring postural equilibrium by producing appropriate adjustments during both self-generated movement and externally applied disturbances, Kathleen Cullen (2008). So finding the proper model of the otolith and semicircular canals can help to understand the characteristics of the vestibular system.

2.1.2 Dynamics of Semicircular canal

Several models are available for the vestibular system. In most of these models, the cupula deflection is modeled as a torsion pendulum. According to R.Ercoline (2004), for an angular acceleration α , the approximate force acting on the cupula can be found from this differential equation(Figure 2.3) :

$$H\alpha(t) = K\theta + \gamma(\frac{d\theta}{dt}) + H(\frac{d^2\theta}{d^2t})$$

H is a mass-dependent, effective moment of inertia of the endolymph and cupula.

α is angular acceleration of head rotation.

K is a position dependent elastic-restoring factor on the cupula.

θ is the angular displacement of endolymph and cupula.

γ is a velocity-dependent damping constant.

t is the time elapsed or time taken.

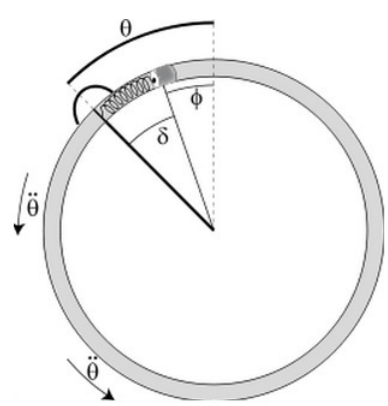

Figure 2.3: Model of vestibular system with cupula. θ is rotation angle of tube [rad] and ϕ is rotation angle of the endolymph inside the tube [rad]. $\delta = \theta - \phi$ is movement between the tube and the endolymph [rad].

Notice that the diameter of lumen of a human vestibular canal is about 0.3 mm, the viscous resistance is high for moderate velocities, and the mass of the endolymph is small. The elasticity of the cupula is small compared with its viscous resistance R.Ercoline (2004). Therefore, the torsion pendulum equation can be simplified as:

$$H\alpha(t) = \gamma(\frac{d\theta}{dt})$$

$$\alpha(t) \propto \frac{d\theta}{dt}$$

H and γ are constants, so after integration with respect to time we have:

$$\omega \propto \theta$$

This means, at the velocities and durations of normal head rotations, the canals act as an integrating accelerometer, R.Ercoline (2004).

Mulder law: According to Mulder (1908), the product of the acceleration and time of application must be equal to 2.5 (Mulders law).

$$\alpha t = 2.5\frac{deg}{s}$$

In fact for weaker angular acceleration (up to a certain threshold limit), perceiving subject must be longer. This limit of perception for angular acceleration is determined not only by the value of the acceleration but also by its time, R.Ercoline (2004).

Thus, if the product αt is found to be a constant from the Mulder law, this strongly supports the existence of an angular velocity threshold δTH, operating on the output

of the torsion pendulum model, as shown in Figure 2.4.

Transfer function form: If we change the upper differential equation of the torsional pendulum to transfer function form, the model will be like a unity gain band-pass filter over the range of $T_L^{-1}\frac{rad}{s}$ to $T_S^{-1}\frac{rad}{s}$, Zacharias (1978):

$$\frac{\hat{\omega}}{\omega} = \frac{T_L s}{(T_L s + 1)(T_S s + 1)}$$

In this model ω and $\hat{\omega}$ are the rotation rate and perceived rotation rate (angular velocity) and T_L^{-1} and T_S^{-1} are lower and upper cut-off frequencies respectively.

Moreover, for lower frequencies, according to Zacharias this can be approximated as a simple washout filter:

$$\frac{\hat{\omega}}{\omega} = \frac{T_a s}{(T_a s + 1)}$$

So if we consider them together we have:

$$\frac{\hat{\omega}}{\omega} = \frac{T_L T_a s^2}{(T_L s + 1)(T_S s + 1)(T_a s + 1)}$$

The threshold δTH (as we can see in the next section), is defined as the lower limit of the possible spectrum of data that the subject can detect, so we have:

$$\Delta = 0 \text{ for } |\delta| <= \delta TH$$
$$\Delta = \delta - SGN(\delta)\delta TH \text{ for } |\delta| > \delta TH$$

where Δ is the output of semicircular canal's threshold, δTH is the semicircular canal threshold value and δ is the cupula deflection in the semicircular canal model, L.D.Reid (1986).

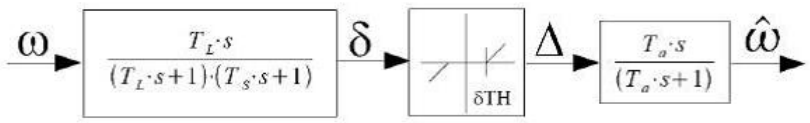

Figure 2.4: Dynamic model of the semicircular channels[Reid and Nahon,1985]L.D.Reid (1986)

In Figure 2.4 the first block refers to the cupula displacement model, that is, the over damped torsional pendulum. The second block represents the human capability of sensing only accelerations higher than a certain threshold and the last block models the washout of human response to steady state rotational acceleration inputs, L.D.Reid (1986).

We can use this control diagram for all dimensional rotations along x,y,z axes with different parameters for the transfer function and dead-zone width Table 2.1.

Frequency Response: The frequency response corresponding to Figure 2.4 is plotted in Figure 2.5. According to Reid and Nahon, it can be seen from the amplitude ratio plot that, this system is a good sensor of angular velocity in the frequency band $0.2\frac{r}{s}$ to $10\frac{r}{s}$ where the response $\hat{\omega}$ tends to zero for both steady-state angular velocity and steady-state angular acceleration inputs.

Table 2.1: The parameters of semicircular model, L.D.Reid (1986).

	Roll(x)	Pitch(y)	Yaw(z)
$T_l[s]$	6.1	5.3	10.2
$T_s[s]$	0.1	0.1	0.1
$T_a[s]$	30	30	30
$\delta TH[\frac{deg}{s}]$	3.0	3.6	2.6

The state space representation of the blocks can be developed as follows, Augusto

(2009):

$$\begin{gathered}\dot{x} = Ax + B\omega, \\ \delta = Cx + D\omega, \\ A = \begin{bmatrix} -(T_l + T_s) & 1 \\ -1 & 0 \end{bmatrix}, B = \begin{bmatrix} T_l \\ 0 \end{bmatrix}, C = \begin{bmatrix} 1 & 0 \end{bmatrix},\end{gathered}$$

and

$$\begin{gathered}\dot{x} = Ax + B\Delta, \\ \hat{\omega} = Cx + D\Delta, \\ A = \begin{bmatrix} -1 \end{bmatrix}, B = [-T_a], C = \begin{bmatrix} 1 \end{bmatrix}.\end{gathered}$$

The given model is nonlinear. This is a problem in terms of computational weight, since it requires linearization.

2.1.3 Dynamics of Otolith Model

Similar to the semicircular channels, several models have also been proposed for the otoliths. Fred and Williams believed that for linear acceleration and the Otolith organ, shearing force acting on the Otolith organ is the product of the excess mass of the statoconia membrane and linear acceleration of the macula, R.Ercoline (2004). So the resistance stemming from the elasticity, viscosity and mass of the otolith system opposes this shearing force:

$$\beta\alpha(t) = Kx + \gamma(\frac{dx}{dt}) + M(\frac{d^2x}{d^2t})$$

where β is the excess mass of the statoconial membrane.

K is elastic resistance,

γ is the viscous resistance,

M is mass and x is linear displacement,

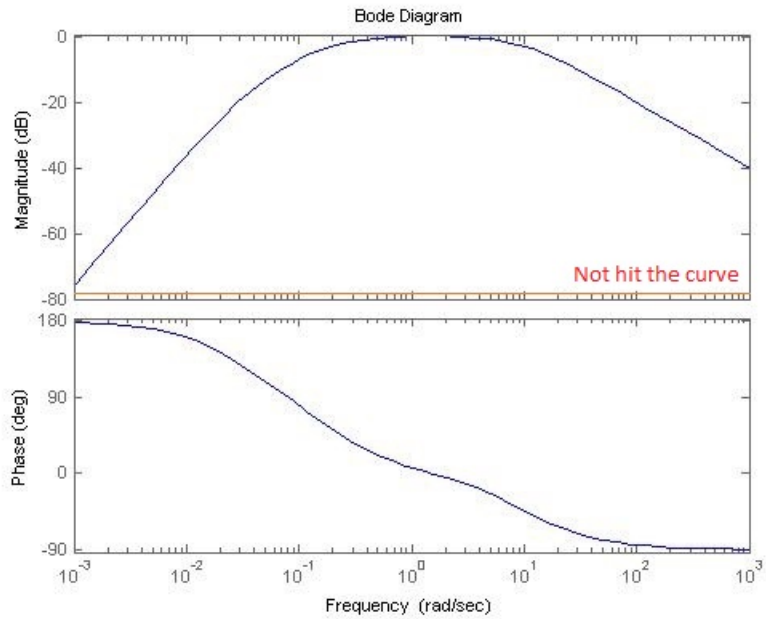

Figure 2.5: Bode diagram of semisircular model

According to the Fred and Williams, the otoliths accurately detect head orientation. However, this ability is modified by habituation during a prolonged stay in the tilted position,that presumably occurs in the central interpretation of the otolith signal.

Transfer function of otolith model: If we represent the model as a transfer function , according to Zocharias if f and $\hat{f}$ are force and perceived force, respectively, along any one of the three axes and $\vec{f} = \vec{a} - \vec{g}$.

$$\frac{\hat{f}}{f} = \frac{K(\tau_a s + 1)}{(\tau_L s + 1)(\tau_S s + 1)}$$

The threshold is represented by:

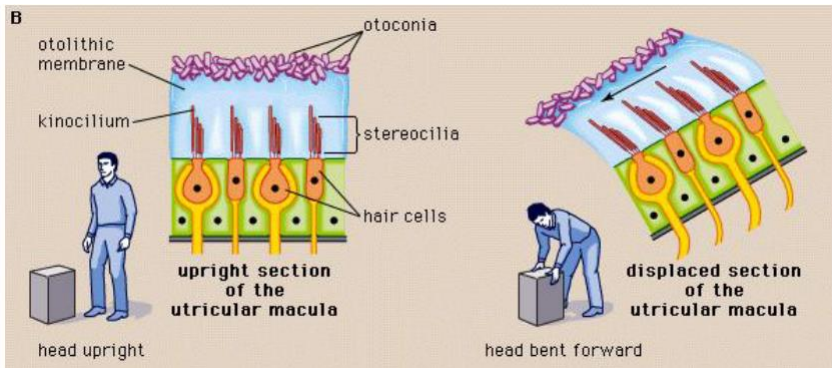

Figure 2.6: The receptor cells of the otoliths organ, Britannica (2009).

$$D = 0 \text{ for } |d| <= dTH$$

$$D = d - SGN(d)dTH \text{ for } |d| > dTH$$

where D is the output of the Otolith threshold, dTH is the Otolith threshold value, d is otolith displacement and τ_L, τ_s , τ_a are otolith vestibular model parameters, L.D.Reid (1986).

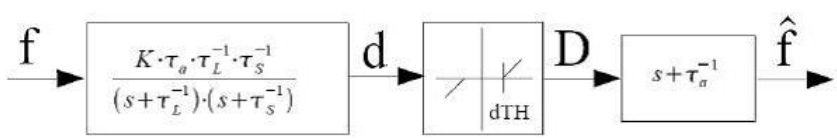

Figure 2.7: Dynamic Model of Otolith,L.D.Reid (1986).

Like the semicircular canal, the blocks in Figure 2.7 illustrate the actual mechanical behavior of the otolith, its mechanical threshold and neural processing activity respectively,L.D.Reid (1986).

The given transfer function represents the perceived specific forces for the Cartesian coordinates and changing the constants will build the three transfer functions

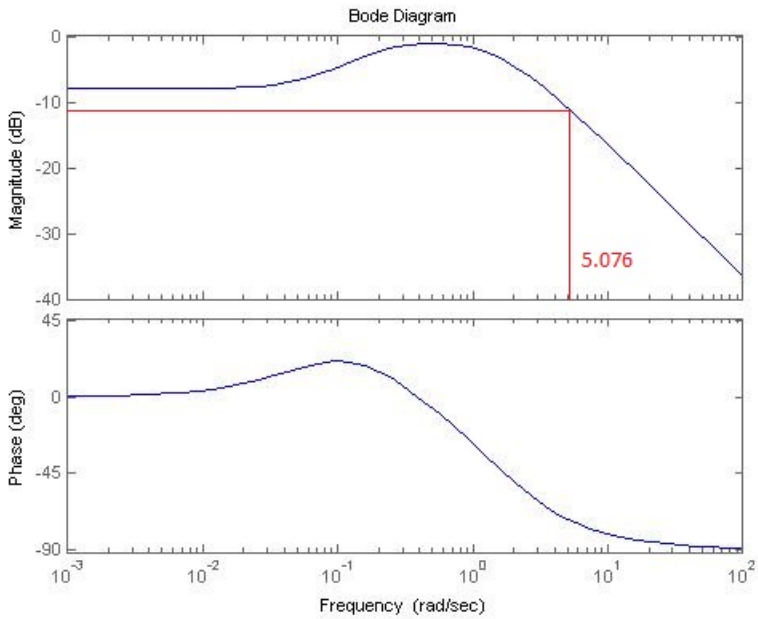

Figure 2.8: Bode diagram of the Otolith model

for each axis x, y , z. The model parameters can be found in Table 2.2 :

Table 2.2: The parameters of Otolith model, L.D.Reid (1986).

	a_x	a_y	a_z
τ_L[s]	5.33	5.33	5.33
τ_s [s]	0.66	0.66	0.66
τ_a[s]	13.2	13.2	13.2
K	0.4	0.4	0.4
$dTH\frac{m}{s^2}]$	0.17	0.17	0.17

Using the canonical form, the following state model can be attained for the first block like the following matrices.

For the last block after the dead-zone, according to Augusto (2009) it is a non-causal system which means the current output of the model has a dependence from

$$\dot{x} = Ax + Bf,$$
$$d = Cx + Df,$$
$$A = \begin{bmatrix} -(\tau_l^{-1} + \tau_s^{-1}) & 1 \\ -\tau_l^{-1}\tau_s^{-1} & 0 \end{bmatrix}, B = \begin{bmatrix} 0 \\ k\tau_a\tau_l^{-1}\tau_s^{-1} \end{bmatrix}, C = \begin{bmatrix} 1 & 0 \end{bmatrix}.$$

the future. In order to deal with this problem, this block will be represented directly in its discretized form, Augusto (2009):

$\hat{f} = \frac{(D_m - D_{mp})}{T_s} + \frac{D_m}{\tau_a}$

where D_{mp} is the previous input of block and D_m is the current input. Just like in the semicircular canals case, the given model is nonlinear.

Bandwidth: According to S.Nice (2004) The bandwidth is defined as the frequency(ω_{BW}) at which the magnitude response curve drops to 70.7% or 3 dB down from its zero frequency value (Figure 2.9). The bandwidth of a two-pole system can be found by finding that frequency for which $Magnitude = \frac{1}{\sqrt{2}}$ (that is, - 3 dB).

For the Semicircular Canal model, if we use the y-axis parameters of Table 2.1 ($T_l = 5.3s$, $T_s = 0.1s$, $T_a = 30s$) and use Matlab to compute bandwidth as you can see in Figure 2.5(magnitude part) there is not any frequency where the magnitude response drops 70.7% down from its zero frequency value.In other words, the model is not valid to determine the bandwidth of the human perception of motion.

$$TF_S = 5.3\frac{30s^2}{(5.3s+1)(0.1s+1)(30s+1)}$$

For the otolith model if we use the parameters for the y-axis in Table 2.2 ($\tau_l = 5.33$, $\tau_s = 0.66$, $\tau_a = 13.2$,$K = 0.4$)and use Matlab to compute the bandwidth as

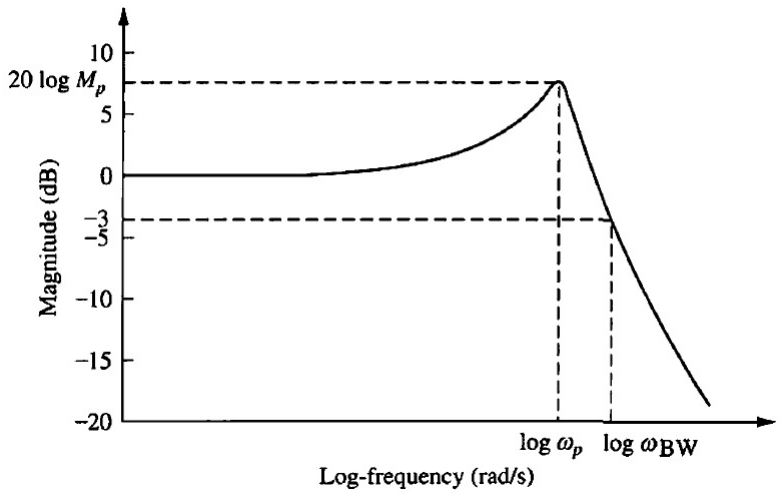

Figure 2.9: Representative bandwith in a sample log-magnitude plot, S.Nice (2004).

you can see in Figure 2.8, we get $\omega_{BW} = 5.0760$.

$$TF_O = \frac{0.4(13.2s + 1)}{(5.33s + 1)(0.66s + 1)}$$

```
>> sys = 5.3*30*s^2/((5.3*s+1)*(0.1*s+1)*(30*s+1))

Transfer function:
             159 s^2
--------------------------------
15.9 s^3 + 162.5 s^2 + 35.4 s + 1

>> bode(sys)
>> bandwidth(sys)

ans =

   Inf
```

```
>> sys=0.4*(13.2*s+1)/( (5.33*s+1)*(0.66*s+1))

Transfer function:
     5.28 s + 0.4
----------------------
3.518 s^2 + 5.99 s + 1

>> bode(sys)
>> bandwidth(sys)

ans =

    5.0760
```

Chapter 3

Psychophysical Threshold

3.1 Introduction

According to the Oxford dictionary, the magnitude or intensity that must be exceeded for a certain reaction, phenomenon, result, or condition to occur or be manifested is called a threshold. Psychophysics usually uses two area of investigation regarding thresholds, detection or absolute thresholds and discrimination thresholds.

Absolute or Detection threshold: According to Strickland (2001), absolute threshold or detection threshold is the minimal amount of energy which is necessary to stimulate the sensory receptors. It can be found with observer analysis or signal detection theory(Section 2.3.1), Gescheider (1997). The general way to find the absolute threshold is to produce a low intensity stimulus and increase it little by little until the subject can detect the presence of the stimulus. In such a task, the subject may undergo many trials before the researcher can determine the threshold. Although the absolute threshold is a useful concept, it does not exist in reality, so in

practice we need to consider a percentage of detection as a scale, Strickland (2001). For example in the case of self-motion, according to Zacharias (1978), motion thresholds are expressed as a minimum detectable motion, determined by some standard psychophysical scale (for example 75% correct detection).

Discrimination Threshold: For a discrimination threshold the participant is asked to describe the magnitude of the difference between two stimuli, or may be asked to detect a stimulus against a background. The magnitude of the smallest difference between two stimuli of differing intensities that the participant is able to detect defference(some proportion of the time (50% is often used) is called the discrimination threshold, Schacter (2010). We will see in the next section how we can use the signal detection theorem for finding discrimination thresholds.

For example in our research we asked our participants to discriminate between forward and backward movement, but for detection, we just needed to discriminate between movement and no movement.

3.2 Different methods of finding thresholds

3.2.1 Non adaptive methods or Classical methods of finding threshold

To test the perception of stimuli three methods are traditionally used,the method of limits, the method of constant stimuli and the method of adjustment, Gescheider (1997).

Method of limits It can be ascending or descending. In the ascending method of limits, some property of the stimulus starts out at a level so low that the stimulus can not be detected, then this level is gradually increased until the participant reports that they are aware of it. In the descending method of limits, this is reversed. In each case, the threshold is considered to be the level of the detected stimuli, Gescheider (1997).

A disadvantage of this method is habituation error, meaning that the subject may become accustomed to reporting that they perceive a stimulus and may continue reporting the same way even beyond the threshold.Conversely, anticipation errors may be made.

Method of constant stimuli In the method of constant stimuli, the levels of stimuli are presented randomly and are not related from one trial to the next. This method prevents the subject from being able to predict the level of the next stimulus, and therefore reduces habituation error, Gescheider (1997) however it is not optimal and sometimes take lots of time to test all random stimuli one by one.

3.2.2 Adaptive methods of finding threshold

According to Treutwin (1995), adaptive methods are more efficient in contrast to classical methods. In adaptive methods, like staircase, the samples are gathered around the threshold point. Adaptive methods mostly are classified into staircase procedures and maximum-likelihood methods.

Staircase procedures In the staircase procedures, we typically start with a high and detectable intensity stimulus. The intensity is then reduced until the subject

make a mistake, at that point we reverse it and intensity is increased until the observer responds correctly, then start another reversal. The threshold is the average of the values of these 'reversals' . There are many different types of staircase procedures, using different decision and termination rules like step-size, up/down rules and number of reversals, Treutwin (1995).

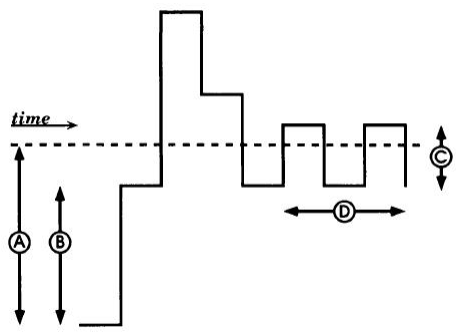

Figure 3.1: The staircase conditions,(A)Starting point (B) Initial staircase step (c) Size of final step (D) Number of reversals,Chris A. Johnson (1999).

In the staircase procedure, as you can see in Figure 3.1, in each series of runs, the following conditions are specified:

- Starting point (e.g.10dB above or below the consumed threshold)
- Size of the initial staircase step (e.g.3-8 dB)
- Size of final step (e.g.2-4dB)
- Number of staircase reversals at the final step size is one to three

For response characteristics, the following are specified:

- The amount of response fluctuation(standard deviation 0-6 dB)

- The number of response errors for each staircase(zero to two)
- Position of response errors in the staircase procedure.

We use the decibel scale (dB) because nearly all human senses obey WeberFetcher's law, that the response of the sense machinery is logarithmic in terms of input intensity, Ross and Murray (1996).

According to Chris A. Johnson (1999), subjects reaction time, the stimulus duration, the inter-stimulus interval, the presentation sequence and the response timing criteria all influence the decision process.

Maximum-likelihood procedures Maximum-likelihood method is similar to staircase procedures. However, the method of choosing the next intensity level is different. In staircase procedure, we only can rely on the previous response which is easier to implement but in Maximum-likelihood methods, we need to consider the whole set of previous stimulus-response pairs in order to have a better result. In a Maximum-likelihood procedure, a prior likelihood is further included in the calculation which is chosen as the best estimate for the threshold and next stimulus, Treutwin (1995).

3.3 Motion thresholds

There is so many works done to find linear and angular motion thresholds. However, due to the greater difficulty to generate linear motion stimuli without adventitious mechanical and acoustical cues, the studies to detect linear motion threshold is much less than angular movement. Moreover the detection of the direction of self-motion also is much higher than without detection of direction, Benson and Stott (1986).

According to Benson and Stott (1986) there have been many papers with different computed threshold values they believed that differences in the orientation of the subjects to the gravitational vector and to the stimulus vector, differences in the tools used to generate the motion stimulus and differences in the psychophysical technique employed can be the reasons for this wide scatter of the experimental data(see Figure 3.2).

Moreover, we have other factors that can influence the absolute threshold, including the observer's motivations and expectations, and whether the person has adapted to the stimulus or not, Strickland (2001).

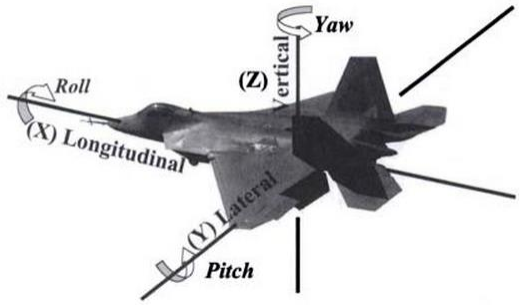

Figure 3.2: Different axes in linear and angular motions, Linear: longitudinal(forward-backward), lateral(right-left), vertical(up-down) Angular: roll, pitch and yaw.

We know that the vestibular system is a multi-sensory organ, i.e. vestibular nuclei receive input and produce output from and to a wide range of cortical, cerebellar and other brain-stem structures. So to measure their function, we can use different methods:

OCR(ocular counter rolling): According to Kingma (2005), body roll is a simple test that changes the orientation of the head and the otolith system. We can measure the responses, such as eye movements in response to a counter roll. Although this method is simple, it is associated with very low sensitivity.

Measure responses to linear acceleration: This method is so popular but according to Kingma (2005), if the sled moved very fast causing substantial motion, so it is important to reduce the movement of the head using a mask. Chris A. Johnson (1999) believe this method may have some irregular responses. A slow reaction time can result in an inadvertent no response. A rhythmic presentation pattern may induce an unintentional yes answer. An essentially long response delay can produce an inadvertent no response to the current stimulus and an inadvertent yes response to the next one.We will call them response anomaly, Chris A. Johnson (1999).

Eccentric rotation: in a human centrifuge device that can rotate up to $7\frac{cycles}{s}$ we can achieve accelerations up to 6G. Ocular (eyes) counter rolling can be measured in this way but it has low sensitivity and detecting the position of the labyrinth is difficult, Kingma (2005).

Table 3.1: Threshold of perception of linear acceleration detected by various scholars Peters (1969) Kingma (2005) A.J.Benson and H.Vogel (1986) Gianna (1996)

Researcher(year)	Motion equipment	Plane of movement	Threshold $\frac{m}{s^2}$
Mach(1875)	Balance	Vertical	0.118
Delage(1888)	Parallel Swing	Horizontal	0.225
Bourdon(1914)	Trolley pulled by falling weight	Horizontal	0.039-0.147
Travis and Dodge(1928)	Oscillating platform	Horizontal	0.029-0.156
Armstrong(1939)	No details	Horizontal	0.019-0.196
Jangkees,Groen(1946)	Parallel swing	Horizontal	0.059-0.147
Lansberg(1954)	Parallel swing	Horizontal(Subject lying on back)	0.089
Graybiel,Patterson(1954)	Human centrifuge	Horizontal(Subject seated upright)	0.265
Benson and Kass (1986)	Linear Osillator motion 0.3 Hz	Vertical and Horizontal	0.077 and 0.029
Spencer,Benson(1986)	Continuous oscillatory stimuli with direction detection for cosine bell velocity trajectory	X ,Y and Z axis	0.063 , 0.057 and 0.154
Gianna (1996)	Bogie mounted on pneumatic wheels,with 7-meter long linear track(Acc Step profile)	Horizontal(Subject seated upright)	0.048
Kingma (2005)	Motor driven linear sled at a stimulus frequency of 1 Hz	Anterior-Posterior and Lateral	0.085,0.085 and 0.065

Chapter 4

Motion cueing and washout algorithms

4.1 Introduction

After the introduction of six-degrees-of-freedom motion simulators, it becomes possible for vehicle simulators to be more mature. In fact they could use advanced motion systems and combine them with faster computers, better and more extended softwares, high resolution images projected over wide screen and so on. The idea was to create a sensation of driving in a real vehicle with the combination of inertial cues, visual and audio cues, Hosman (1999).

This is a difficult task because the hardware displacement is limited. Therefore, vehicle signals cannot be sent directly to the motion platform and a motion cueing is required. In fact as the motion base moves closer to its physical limits, the algorithm should reduce the amount of additional motion commands. As the motion base returns to its center, it is adjusted to allow more motion. There are several well-known

conventional techniques applied for computation of motion cues named washout filters Augusto (2009). A strategy to reproduce the signals perceived by the driver in real driving is the aim of a motion cueing algorithm.

One of the important factors in motion cuing is using other cues like vision. We know that perception of body orientation in space can be influenced by vision so if we can use a tilted full visual surrounded screen, the illusion is even better. According to Daniel R. Berger (2007) visual cues have more influence on the perceived orientation than the sensed direction of gravitation. They call this phenomenon vection (visually induced illusion of rotational or linear self-motion).

The start of vection is delayed for a few seconds after the start of the stimulation because of vection latencies, Jean-Claude Lepecq and Baudonniere (1999). They found in vertical movement there is a negative correlation between individual vestibular threshold and vection onset latency-the lower the vestibular threshold, the longer the delay in vection, Jean-Claude Lepecq and Baudonniere (1999).

The structure of a system with motion cueing described in Figure 4.1 .

According to Daniel R. Berger (2007) the majority of cueing algorithms use a short initial forward surge motion with a backward tilt of the platform that presses the participant into the seat, meaning that the body's angular velocity is under the threshold and cannot be detected by the vestibular system. In fact, the surge translation should have an acceleration above the sensory threshold and a deceleration below the threshold.

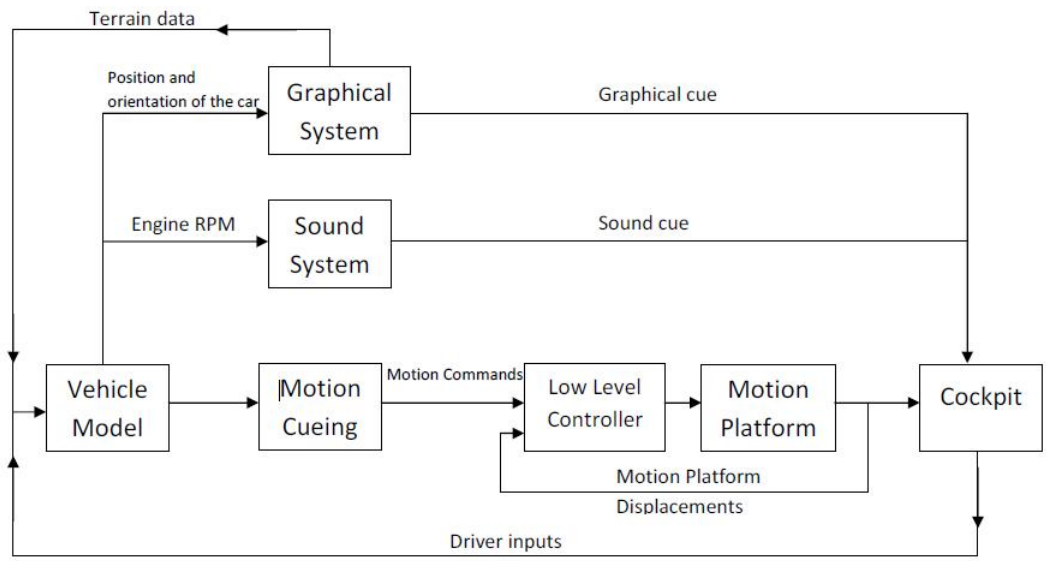

Figure 4.1: Scheme of driving simulator, Augusto (2009)

4.2 Tilt coordination

We know that the combination of inertial force and gravity yields a gravito-inertial force vector, see Figure 4.2. According to, R.Ercoline (2004), to simulate this force we can tilt the platform-tilting is a technique applied by the washout filters in order to simulate sustained acceleration. This method uses one important feature of the Otoliths organ, their ambiguity and inability to distinguish translational acceleration from gravity, Augusto (2009). As can be seen in Figure 4.2, the force in forward acceleration with the head upright can be similar to constant velocity with the head tilted up.

According to Augusto (2009), when we tilt the platform, depending on the rotation, the gravity vector will develop components along the X and Y axes. These components are perceived by the driver as translational accelerations and the driver

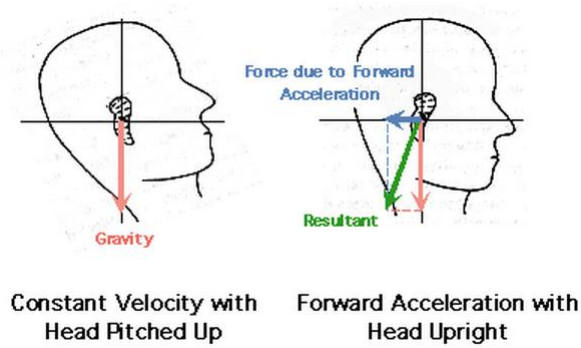

Figure 4.2: Ambiguity of Otholith system. Bankslap (2009)

should feel that he is driving in a real vehicle. The important point is generating tilt without making false cues, so the tilt rate should not be more than the threshold, Telban and Cardullo (2005). In fact, to make backward tilt we need to align the simulated gravito-inertial force vector with the direction of gravity. It makes the observer interpret the rotation of this vector as a forward acceleration, see Figure 4.4.

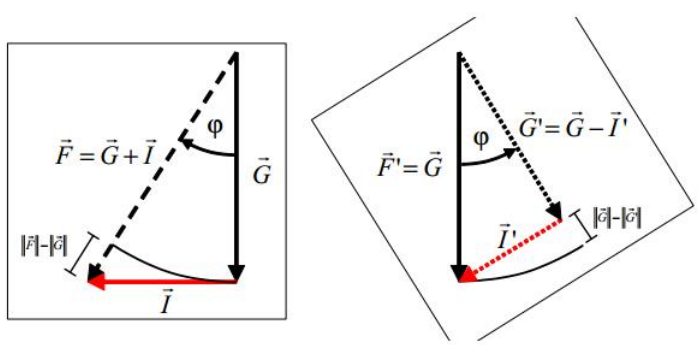

Figure 4.3: Make backward tilt to interpret forward acceleration.

In the left part of Figure 4.3 during a real acceleration , the resulting force vector F is the sum of the gravitational force G and inertial force caused by acceleration (I).

To simulate the acceleration (a) we can find angle φ and rotate the platform by this angle so that the gravitational force vector G points in the direction of the simulated force F' , Daniel R. Berger (2007).

$$\varphi = \arctan(\frac{I}{G}) = \arctan(\frac{a}{9.81})$$

Moreover a fraction of the gravitational vector can be perceived as a linear self-motion acceleration of magnitude $g \sin(\varphi)$.

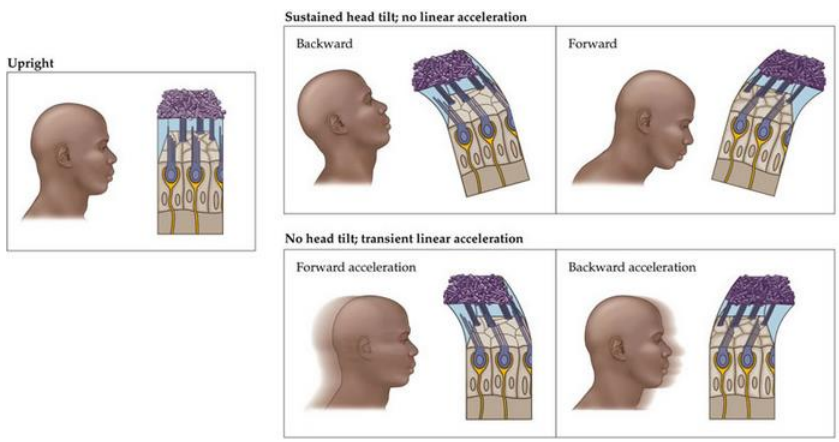

Figure 4.4: Linear acceleration with and without tilt, Jeremy M. Wolfe (2012).

4.3 Different motion cueing algorithms

4.3.1 Non predictive cueing algorithms

In non predictive cueing algorithms or washout filters the basis is to compute the acceleration of the platform by high-pass filtering the corresponding vehicle acceleration and removing the low-frequency component of vehicle acceleration. This can be

done along any degree of freedom and to maintain the platform limitations we need to tune the filters, Mehmet Dagdelen (2009).

According to Colombet (2008), we have three different washout algorithms to drive the simulator: classical, adaptive and optimal washout algorithms.

Classical: A classical algorithm is simply based on frequency domain's trade-off and platform command results from high-pass filtering of the vehicle acceleration.

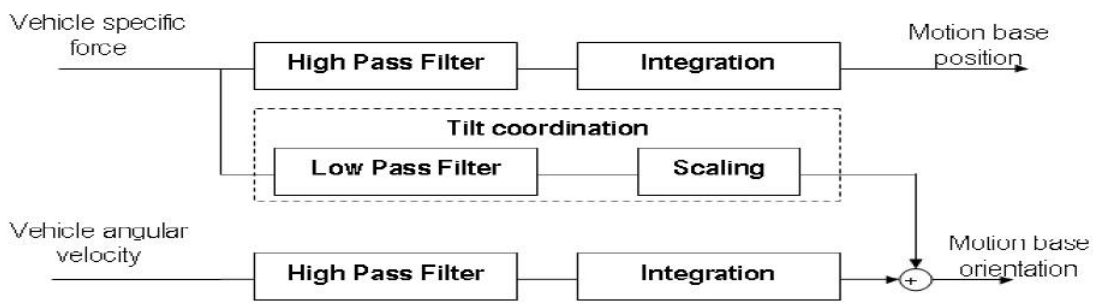

Figure 4.5: Classical motion cueing algorithm, Colombet (2008)

In this motion cueing strategy, the washout filter can be used in a very general way. The vehicle's linear and angular accelerations are high-pass filtered using second order filters to maintain the motion system in its workspace. Another third order filter is applied to washout to a neutral position. Moreover the vehicle accelerations are specially low-pass filtered, scaled and passed through rate limiters to produce additional pitch and roll tilt angles. So we have three parts: rotational, translational and coordination channels, Augusto (2009).

We use high-pass filters to eliminate low-frequency, high-amplitude motions of the vehicle and extract the transient components of the acceleration , Harry J. Zywiol (2003). And also provide tilt coordination in order to recover some of the low

frequency acceleration cues which lost, due to the high frequency filtering, Harry J. Zywiol (2003).

The only part that remains in this scheme is to set the filters' parameters: cut off frequencies and gains. In fact the selection of the parameters for the digital filters is a trade-off between maximizing cue recovery and eliminating motion commands that are outside the motion limits. In the classical method the parameters are usually adjusted by simple trial and error experiments. Consequently, this method does not lead to an optimal result for any given situation and is inflexible, Augusto (2009).

Adaptive method In adaptive method is like a classical algorithm but cut-off frequencies of the filters are not constant and are varied in real time to minimize the cost of platform excursion and acceleration gap, Harry J. Zywiol (2003).

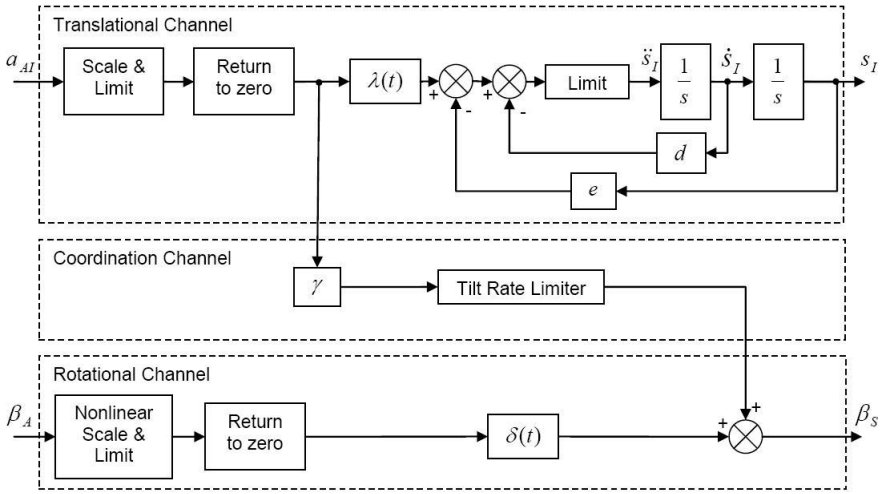

Figure 4.6: Adaptive washout filter, Telban and Cardullo (2005)

As you be seen in Figure 4.6, the values of λ and δ are time varying and are changed at every step but γ, e and d are fixed weights. In order to compute the time

variant weights, an optimization problem needs to be solved on-line. According to an objective function that compensates for the error between acceleration and rotation in the car and the motion platform, it can be done normally or using a fuzzy-based algorithm to use more parameters for the optimization problem, Khaled Fellah and Morsly (2013).

In fact, the difference between adaptive and classical methods is in the washout filters such that it allows a better utilization. However, in spite of providing the platform with an optimal input given a specific set of states, this strategy can not give a good sensation of movement. In fact it would be better if instead of focusing in reproducing the vehicle dynamics, we focus on duplicating the sensations experienced in the car. The optimal method can help to produce real sensations, Augusto (2009).

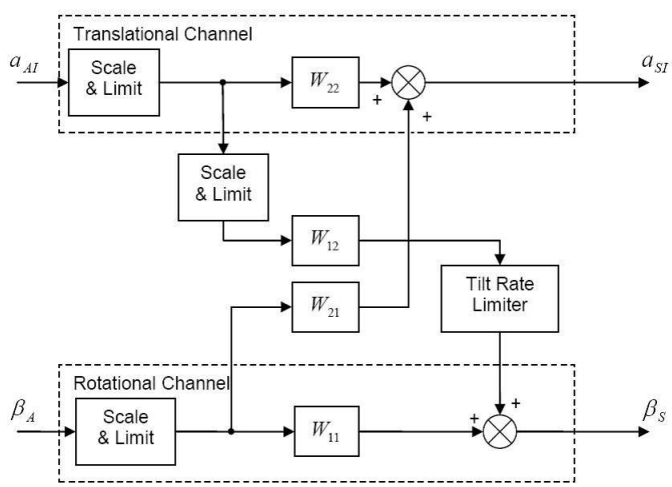

Figure 4.7: optimal washout filter, Murgovski (2007).

Optimal method In an optimal algorithm a linear model of the vestibular system is used. The challenge is now to establish a model that relates the accelerations

and rotations of the vehicle with the ones that should be applied, see Figure 4.7. A cost function is defined that includes terms that attempt to create the same motion sensation in the simulator, based on the linear model of the vestibular system. In solving the problem we can use Riccati equations to find optimal linear acceleration and angular velocity,Harry J. Zywiol (2003).

4.3.2 Model Predictive Control based motion cueing

Model predictive control(MPC) is an advanced control technique which we can use in motion cueing algorithms. In MPC, as can be seen in Figure 4.8, the idea is to have a reference trajectory $r(t|k), t >= k$ (in discrete-time), and a current measure of the output $y(k)$ to predict the future output corresponding to the input sequence in a time-window of length N_p (prediction horizon length) (Figure 4.8). Then we compute the input sequence that minimizes the following cost function(minimization problem) Alessandro Beghi (2012).

$\epsilon(k+i|k) = r(k+i|k) - y(k+i|k)$

One of the implementations of MPC uses the state space models. A common discrete state space model is given as,Wang (2009):

$x_m(k+1) = A_m x_m(k) + B_m u(k)$

$y(k) = C_m x_m(k)$

where u is the input, x is the state and y is the output. For convenience we assume that the input does not have a direct effect on the output. According to Wan Wang (2009), we can consider the state difference $\Delta x_m(k)$ when we have input difference $\Delta u_m(k)$ so we can write:

$\Delta x_m(k+1) = A_m \Delta x_m(k) + B_m \Delta u(k)$ (I)

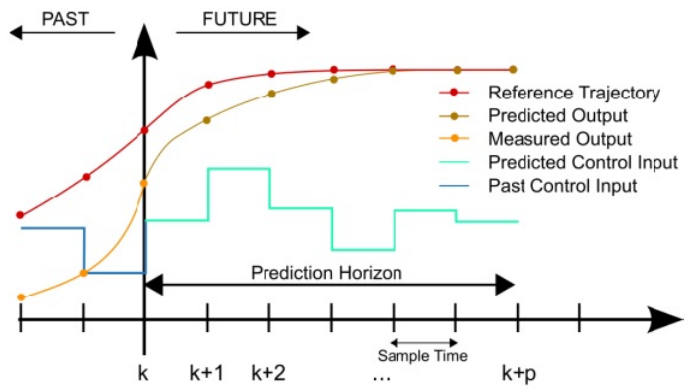

Figure 4.8: Model Predictive Control base motion cueing [Alessandro 2012]Alessandro Beghi (2012)

Note that the input to the state-space model is $\Delta u(k)$. The next step is to connect $\Delta x_m(k)$ to the output $y(k)$. To do so, a new state variable vector is chosen to be

$x(k) = [\Delta x_m(k)^T y(k)]^T$

where the superscript T indicates matrix transpose.

with considering the output difference we have:

$y(k+1) - y(k) = C_m A_m \Delta x_m(k) + C_m B_m \Delta u(k)$ (II)

from (I) and (II) we can get:

$$\overbrace{\begin{bmatrix} \Delta x_m(k+1) \\ y(k+1) \end{bmatrix}}^{x(k+1)} = \overbrace{\begin{bmatrix} A_m & o_m^T \\ C_m A_m & 1 \end{bmatrix}}^{A} \overbrace{\begin{bmatrix} \Delta x_m(k) \\ y(k) \end{bmatrix}}^{x(k)} + \overbrace{\begin{bmatrix} B_m \\ C_m B_m \end{bmatrix}}^{B} \Delta u(k)$$

$$y(k) = \overbrace{\begin{bmatrix} o_m & 1 \end{bmatrix}}^{C} \begin{bmatrix} \Delta x_m(k) \\ y(k) \end{bmatrix},$$

consider that $o_m = [000.....0]$. We call the triple (A, B, C) the augmented model,

Wang (2009). So we need to find the augmented model from the main model.

Part II

Method and Findings

Chapter 5

Our method

5.1 Introduction

In this project we implemented a motion cueing algorithm using C++ under Linux to generate linear motion stimuli. The program can simulate forward or backward motion with a visual attention cue at the start of each trial and has a mechanism to gather the participant's response. We also added white noise to mask mechanical auditory cues. Moreover, we generated vibration for each trial to simulate a noisy environment close to real driving or flying.

The motion-generating procedure uses a non-adaptive approach (classical method of constant stimuli) (Section 3.2.1), in which the levels of stimuli are presented randomly and are not related from one trial to the next. As we saw in previous chapters, this method takes longer in comparison to adaptive methods like staircase procedures since we were testing all accelerations for every individual experiment. On the other hand, this method prevents participants from being able to predict the level of the next stimulus. Therefore this procedure reduces habituation error, Gescheider (1997).

In our experiments we are using accelerations between $0.01 \sim 0.2\frac{m}{s^2}$ forward and backward. The program starts by making an array of accelerations (acceleration profile in Table 6.3) that are shuffled before executing the main loop, Figure 5.6. Notice that we are using an array of constant accelerations and start the motion with these values. But due to the fact that the simulator is a mass in our system and acts as a low pass filter, it can disturb our acceleration values. To address this we are using two different accelerometers, AC and DC, to get precise acceleration values and to avoid losing any information (we will describe it more in the next section).

Figure 5.1: Hexapod McMaster motion simulator v. Mohrenschildt (2010)

5.2 Technical equipment and restriction

As can be seen in Figure 5.1 our simulator is equipped with a spaceship-pod fiberglass shell, a visual system consisting of three 42" flat screens to give a 120 degree field of view and Dolby digital surround-sound. The motion system is electric and has six-degrees-of-freedom (surge, sway, heave, roll, pitch, yaw) with a Steward platform

Maximum Velocity		Maximum Acceleration		Maximum Excursion		
					Single	Maximum
Surge	± 0.50 m/s (± 19.7 in/s)	Surge	± 6.0 m/s² (± 0.61 g)	Surge	± 0.25 m (± 9.8 in)	± 0.27 m (± 10.6 in)
Sway	± 0.50 m/s (± 19.7 in/s)	Sway	± 6.0 m/s² (± 0.61 g)	Sway	± 0.25 m (± 9.8 in)	± 0.26 m (± 10.2 in)
Heave	± 0.30 m/s (± 11.8 in/s)	Heave	± 5.0 m/s² (± 0.51 g)	Heave	± 0.18 m (± 7.1 in)	± 0.18 m (± 7.1 in)
Roll	± 30.0 °/s	Roll	± 500 °/s²	Roll	± 21.0 °	± 22.0 °
Pitch	± 30.0 °/s	Pitch	± 500 °/s²	Pitch	± 22.0 °	- 23.0 ° / + 25.0 °
Yaw	± 40.0 °/s	Yaw	± 400 °/s²	Yaw	± 22.0 °	± 23.0 °

Table 5.1: Data sheet of MB-E-6DOF/12/1000KG ,Moog (2014)

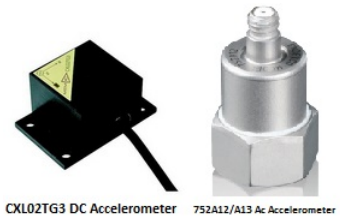

Figure 5.2: DC response and AC response accelerometers used in the system

(Moog 6DOF2000E) with a 1000 Kg (2,205 lbs) payload, and a maximum of $0.6G$ or $5.88\frac{m}{s^2}$ of acceleration(See Table 5.1). We installed two different accelerometers, DC and AC response (CXL02TG3 and Endevco 752A12/A13 respectively, Figure 5.2), within and beneath the platform to achieve a realistic acceleration and not losing any information regardless of filtering the simulator itself.

Unwanted tilt On the Steward platform we always have an unwanted tilt on the edges, see Figure 5.4. Sometimes this tilt is more than the motion threshold. Especially for higher accelerations close to maximum (Table 5.1), participants can become aware of this unwanted motion. To solve this we only use 60 percent of the maximum length limit.

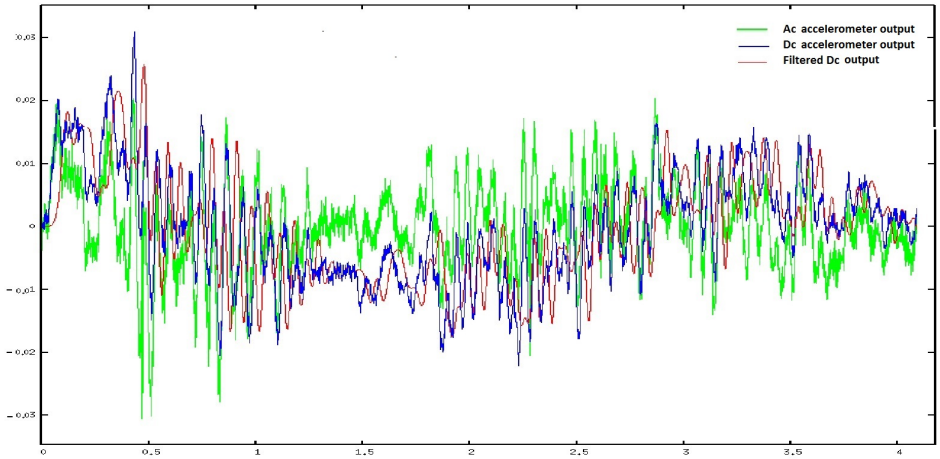

Figure 5.3: Output signals of DC and AC response accelerometers. We are using AC and DC response accelerometers together to not lose any information regarding filtering.

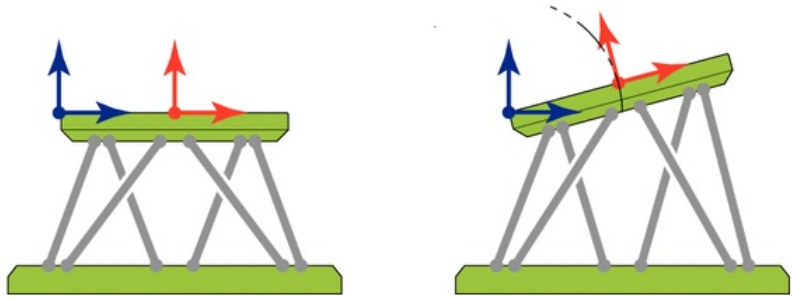

Figure 5.4: Unwanted tilt on the edges, NewPort (2009).

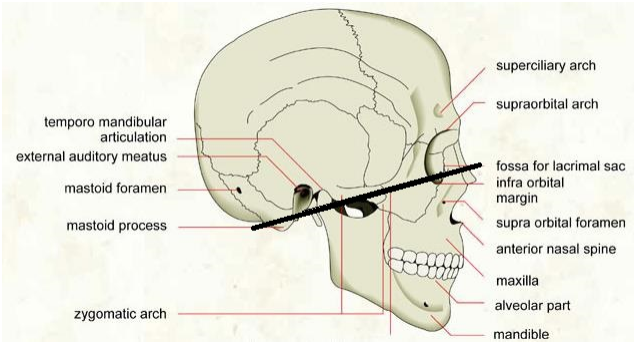

Figure 5.5: Best angle to detect threshold, R.Ercoline (2004).

Best head angle: According to R.Ercoline (2004), tilting of the head from the vertical position will bend some cilia of hair cells and produce stimulation. To get the best result, subjects can be fixed to the cabin with a harness. We need to adjust head orientation so that a line joining the infra-orbital margin and external auditory meatus is tilted downwards 30° relative to earth horizon. It also has less effect when the head is tilted close to and beyond 90° to the vertical axes.

In our project we tried to simulate the situation very similar to real driving or flying so we did not consider any constraints for head angle.

5.3 Procedure

As you can see in Figure 5.6, the procedure starts by initializing constraints such as maximum movement, washout acceleration and present-phase-time. It then generates white auditory noise and shuffles the vector of accelerations (acceleration profile in Table 6.3) before using them in the program core. We can describe the program in three parts:

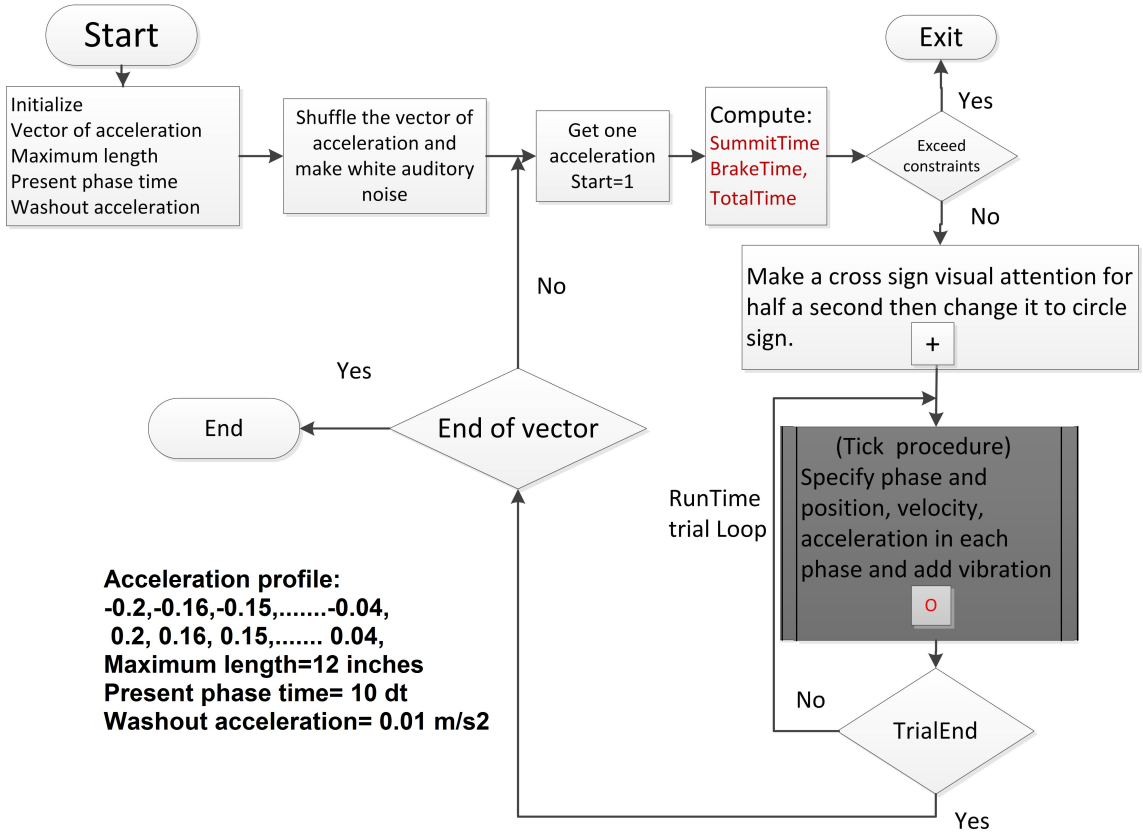

Figure 5.6: Data flow diagram of the program: As you can see in the main loop for each block we have a visual attention cue which is shown by a cross and circle picture in the screen.Notice that the boolean variable Start shows the start of trial and TrialEnd shows the end of the trial. The variables SummitTime, BrakeTime and TotalTime are computed for each trial once individually before going to the inner runtime loop.

- Motion cueing
- Visual attention cue
- Making vibration

5.3.1 Motion cueing algorithm

The purpose of the cueing algorithm is to give a sensation of motion by running the platform with a constant acceleration and washout after a specific duration (PRESENT_Phase_Time). Our program generates and sends data to the simulator in discrete time with frequency of 60Hz ($dt = \frac{1}{60} = 0.0166s$).

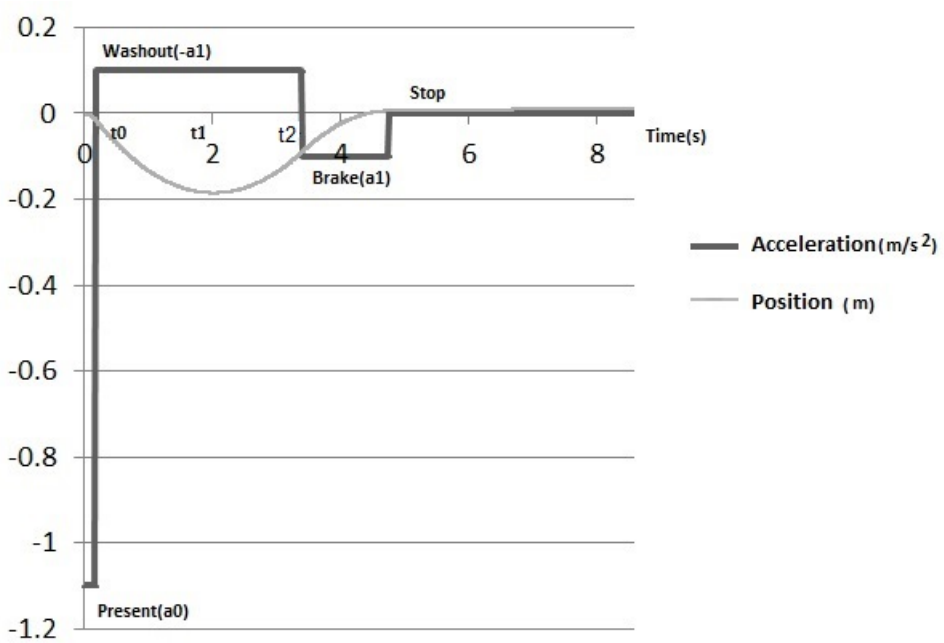

Figure 5.7: Different phases for $acc = -1.1\frac{m}{s^2}$. We can see 4 phases PRESENT, WASHOUT, BRAKE and STOP, PRESENT_Phase_Time=10dt=0.166 s

For our algorithm we have four distinct phases which we call PRESENT, WASHOUT, BRAKE and STOP, see Figure 5.7.

- PRESENT: Running the platform with present acceleration for a specific time of PRESENT_Phase_Time which is equal to $10dt = 0.166s$
- WASHOUT: Change the acceleration to the constant washout acceleration to decrease the speed and stop before exceeding the maximum length limit.
- BRAKE: Change the sign of washout acceleration when the position becomes half of maximum in order to brake and get back smoothly to the initial position.
- STOP: Stop the platform before starting the next trial.

Computing the timing variables and constraints

Our program generates data for the simulator every $dt = 0.016$ seconds, so the best way to switch from one program phase to the next is to use timing variables. In fact we can check these timing variables to specify program functionality. Notice that because data is sent to the simulator at discrete times, we always need to consider time quantization in our timings. It means we always need to use the ceiling of the timing values with considering the sampling period and frequency to make it a factor of dt. We wrote a quantize function which always compute the ceiling of values like the following.

```
double quantize(double t)
{
double st=Ceil(t*60.0);      // 60.0 is the frequency of sampling
return(st*DT);               //DT is sampling period
```

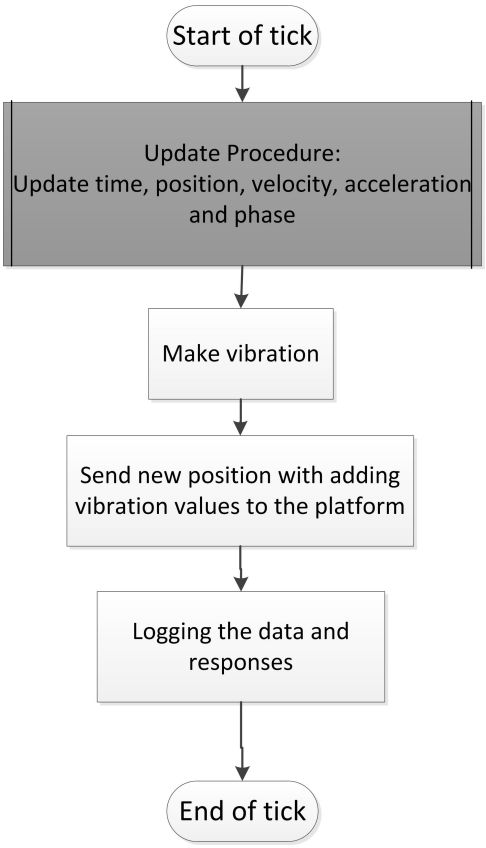

Figure 5.8: Different steps in each tick(inner runtime loop). The procedure is repeated with frequency of 60 hertz, $dt = 0.0166s$.

```
}
```

We can define these timing variables as follows:

- SummitTime: Specific quantized time when the platform is in the washout phase and has maximum displacement.
- BrakeTime: Specific quantized time when the BRAKE phase is started. We need to negate washout acceleration.
- TotalTime: Amount of time from start to end of each trial including PRESENT, WASHOUT and BRAKE phases.

Computing the SummitTime, BrakeTime and Total time: As can be seen in Figure 5.9, we run the platform with a present acceleration a_0 until time $t_0(PRESENT\_Phase\_Time$ $10dt)$. We then switch to acceleration a_1 in the $WASHOUT$ phase. We then reach the maximum at time $t1$(SummitTime) and following that, we switch to the $BRAKE$ phase at time $t2(BrakeTime)$ with a negated washout acceleration for the final braking and eventual $STOP$ at the end for StopPhaseTime duration.

We know in Figure 5.9 after passing the duration(PRESENT_Phase_time) the speed and position are:

$y_0 = \frac{1}{2}a_0t_0^2$ (Displacement at t_0)

$v_0 = a_0t_0$ (Velocity at t_0)

To find the summit time, according to the Time Independent Kinematic Motion Equation we have:

$v_1^2 = v_0^2 + 2a_1(y_1 - y_0)$

we know that in the summit point $v_1 = 0$ so after substitution:

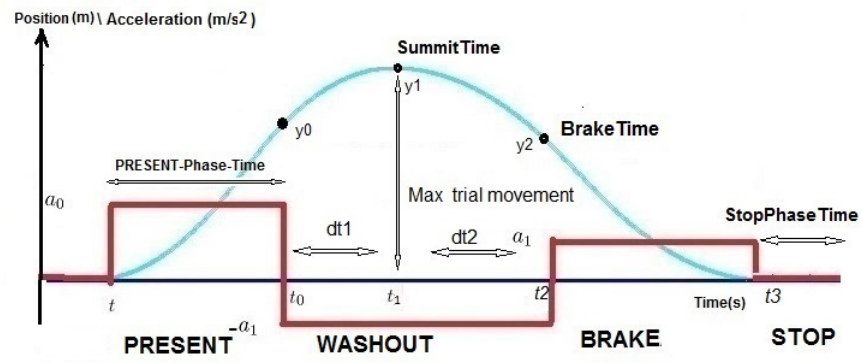

Figure 5.9: Cueing algorithm phases. In the picture t0,t1,t2 are washout, summit and brake times respectively.

$y_1 = y_0 - \frac{v_0^2}{2a_1}$ (maximum position in washout phase)

Notice that for positive accelerations the washout acceleration(a_1) is negative and for negative accelerations is positive.

To find the summit time, according to the Kinematic Velocity Equation, we have:

$v_1 - v_0 = a_1 dt_1$

So the time duration to get maximum position is $dt_1 = -v_0/a_1$ and after quantization and adding to t_0 we have:

$SummitTime = t_1 = quantize(t_0 - v_0/a_1)$

Notice that to avoid exceeding movement constraints we always compute the maximum position for constant washout acceleration a_1 before running the Tick procedure and it always has to be less than MaxLength, see Figure 5.6.

Moreover, as we saw before we switch to the $BRAKE$ phase when we are at half of the maximum movement ($\frac{y_1}{2}$) so to find the brake time we have:

$y_2 = \frac{y_1}{2}$

According to the Basic Kinematic Motion Equation we have:

$y_2 = y_1 + v_1 t + \frac{1}{2} a_1 dt_2^2$ (The Basic Kinematic Motion Equation)

As $v_1 = 0$ and $y_1 = 2y_2$ we have:

$dt_2 = quantize(\sqrt{\frac{-2y_2}{a_1}})$

and:

$BrakeTime = t_2 = quantize(dt_2 + t_1)$

Finally to find the TotalTime we know that in Figure 5.9, the time to move from y_1 to y_2 is equal to the time to move from y_2 to the initial position so we have:

$TotalTime = t_3 = quantize(t_2 + dt_2)$

Euler method of approximation: We are generating the positions at discrete time steps with frequency of 60 Hz, where the time interval is determined by $\Delta t = 0.0166s$. According to the Euler method of approximation:

if $y'(t) = f(t, y(t))$ we can write

$y(t + \Delta t) \approx y(t) + \Delta t f(t, y(t))$

To update the position over time, we are using velocity, and acceleration which are modeled as functions of time, $v(t)$, $a(t)$, respectively. We have

$\frac{dv}{dt} = a(t)$, $\frac{dx}{dt} = v(t)$

The position $x(t)$ is updated by its velocity $v(t)$ as in the following equation:

$x(t + \Delta t) = x(t) + \Delta t v(t)$

The velocity $v(t)$ is updated by its acceleration $a(t)$ through:

$v(t + \Delta t) = v(t) + \Delta t a(t)$

5.3.2 Visual attention cue

As we saw in the main data flow diagram (Figure 5.6), in order to specify the start of each trial in our program, we created a visual attention cue which is shown as a

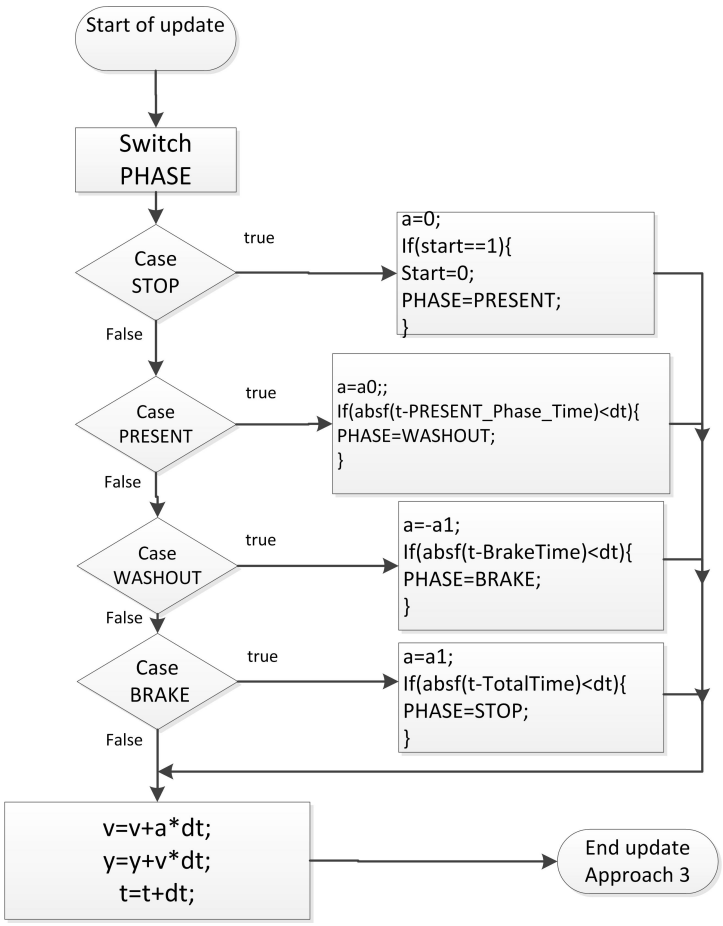

Figure 5.10: Block diagram of update block. In this diagram a0 and a1 are the present and washout acceleration respectively. To go to next phase we always use BrakeTime and TotalTime we compute them once. Position(y), velocity(v) and time are computed in each tick from the Euler method of approximation in the last block

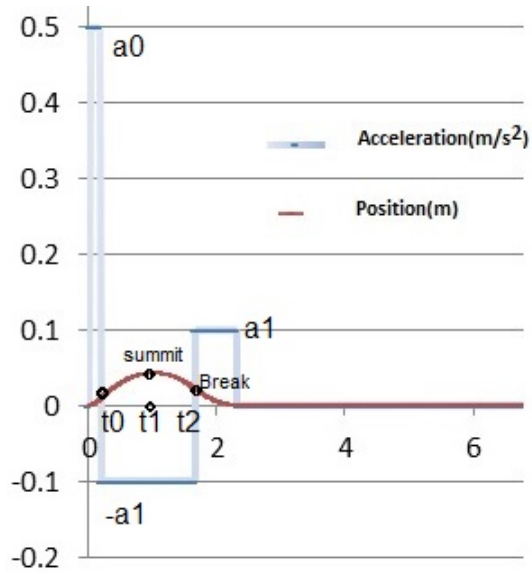

Figure 5.11: Different phases for Acc=$0.5\frac{m}{s^2}$.

small cross sign in the screen for half a second and changes into a circle sign at the beginning of each trial, see Figure 5.13.

5.3.3 Generating vibration

According to G.McConnell (2014), vibration is a mechanical phenomenon whereby oscillations occur about an equilibrium point. To make it random we need to move non-deterministically. It means that future behavior cannot be precisely predicted. Some common examples of random vibration include an automobile riding on a rough road, wave height on the water or the load induced on an airplane wing during flight.

To make vibrations in our simulator the most popular way is to use the Sinusoidal or Sine Vibration method with phase modulation, DES (2013). In this method we are using a *sin* function with random variables for the parameters. The parameters used

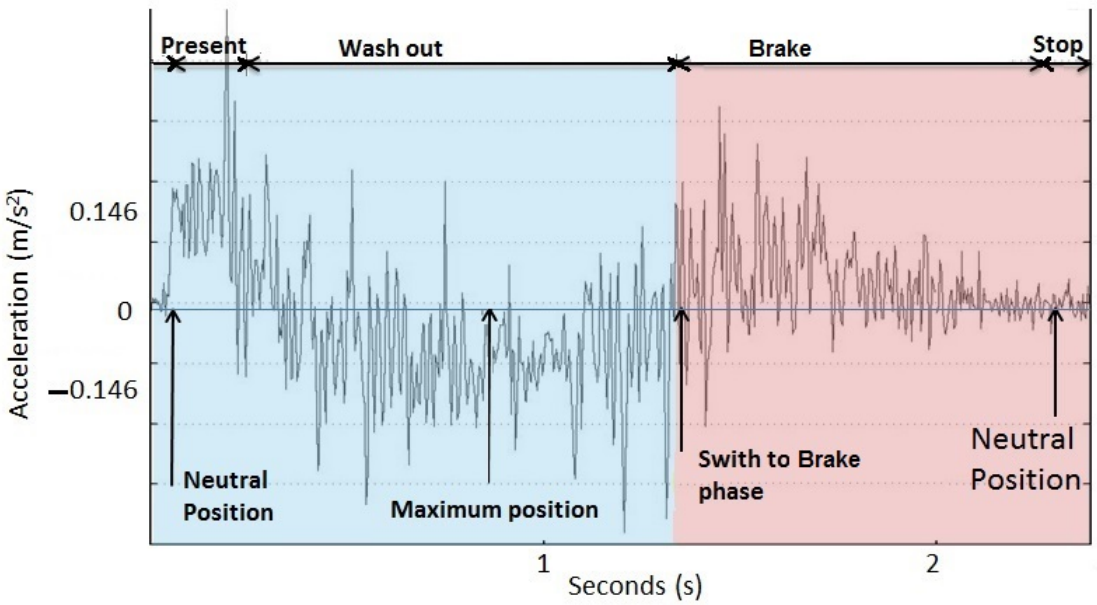

Figure 5.12: Accelerometer output for $0.146\frac{m}{s^2}$

to define sinusoidal vibration are amplitude(A) (usually acceleration or displacement), angular frequency (w), phase (phi)and shift parameter(B). We also defined another constant scale factor to limit the overall value of vibration(S).

Vibration value=$S(Asin(wt + phi) + B)$

In our algorithm the amplitude(A) and scale factor(S) are constant. At any time period (60Hz) we have discrete phase(phi) and shift factor(B).

In our program, the range of our variables are: $Phi \subset [0, 0.1)$ and $B \subset [0, 0.5)$ and constants are $A = 0.02$ and $S = 0.2$. With considering these variable constraints we can make a random vibration between [0,0.104) meters in each proportion of time, see Figure 5.14.

Notice that for a linear movement in the x axis we create vibration signals in two

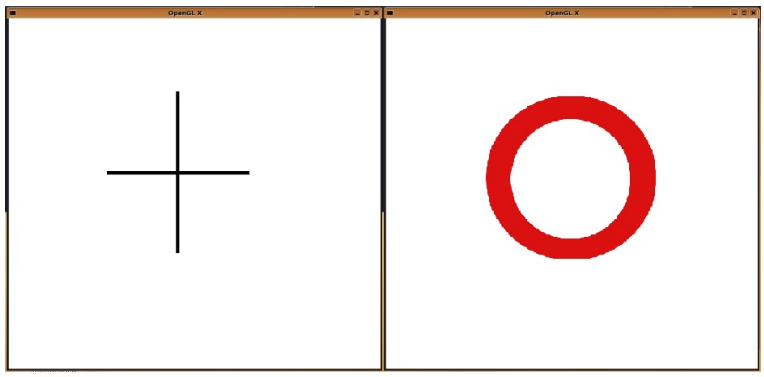

Figure 5.13: Cross symbol initiates beginning of trial while a circle indicates trial has commenced

other directions (y, z). In fact we do not want to disturb the linear motion of direction x (in this case), with vibration, see Figure 5.15.

The flowchart of making noise in the x direction is shown in Figure 5.16.

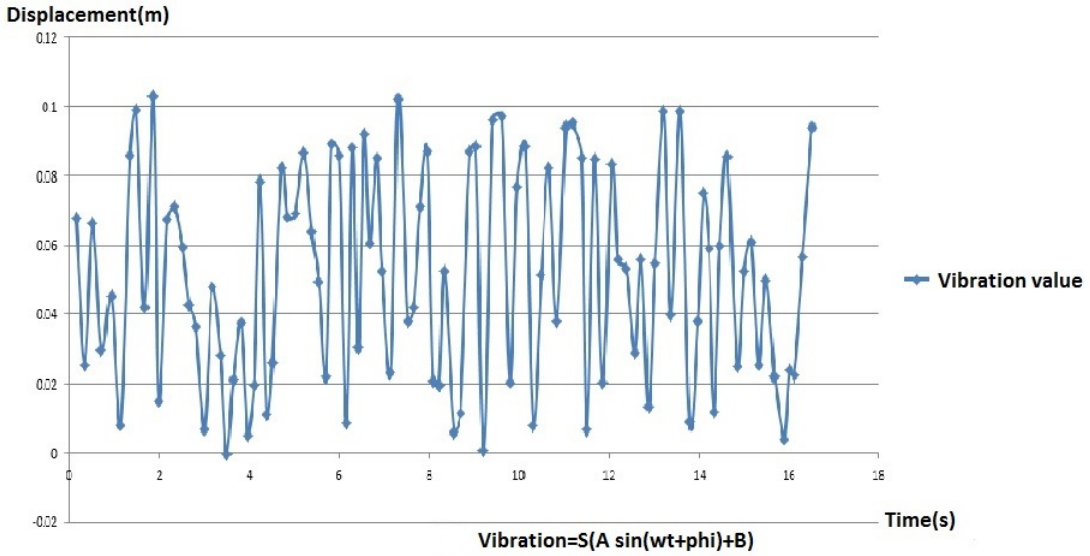

Figure 5.14: Random vibration signal generated by program with considering random Phase and random shift factor

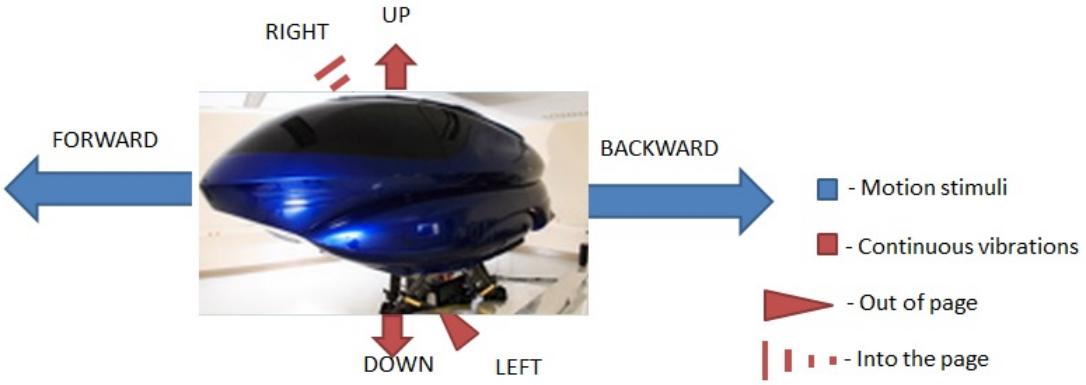

Figure 5.15: Motion stimuli and vibration axis

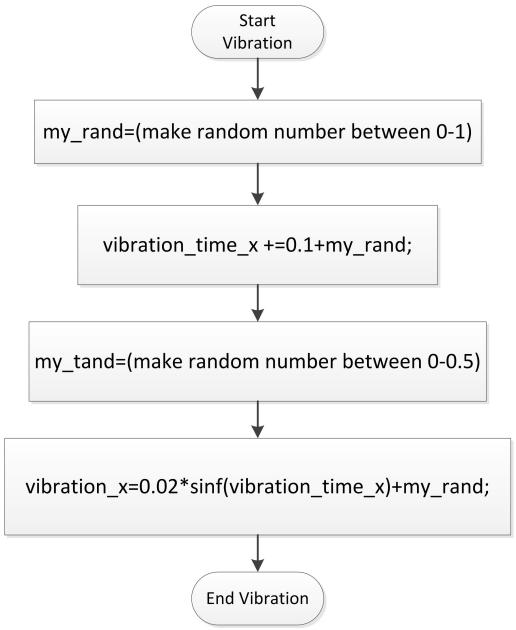

Figure 5.16: Flowchart of making vibration when platform is moving in x direction.y and z directions are the same as x. As you can see in second block the vibration time is increased randomly. Moreover the vibration_y and vibration_z are added to the position in each tick when we are moving in the x direction.

Chapter 6

Findings

6.1 Introduction

In this chapter we will describe the analysis which we did on the collected data after our experiments. For each experiment we used participants who did not have any clinical abnormality with their vestibular system.They were mostly at either undergraduate or graduate levels of study. The participants sat inside the motion simulator on a leather car tactile and wore ear plugs to decrease unwanted auditory cues. We ran the motion cueing program and asked them to respond and detect the direction of linear motion in the system, see Figure 6.1. We collected and stored the responses (Acceleration, Response time, Pressed key status) in a log file to process them later, see Table 6.1.

The Pressed Key status shows correctness of a subject's responses and has three cases:

- Participant can not detect the motion.

Figure 6.1: Using leather car seat as tactile and wearing ear plugs inside the platform

Table 6.1: The data which logs in program

	Logging time	Contents
Response data	After response or at the end of trial for no-response	Acceleration, Response time, Pressed key status

- Participant detects the motion with the correct direction.
- Participant detects the motion with the wrong direction.

We tested the program for 4 participants (4 different time sessions, 4 blocks/session), 168 trials/block and stored the responses. In order to find the vestibular system characteristics and analyze the data, we used statistical hypothesis testing and signal detection theory, explained in the next section. We tested the accuracy and the response time for these participants and results indicated that participants can reliably discriminate the motion direction within a noisy movement environment, resulting in decreased thresholds across sessions.

Before going into the details of the analysis, we first try to describe the appropriate

signal detection theory.

6.2 Signal Detection Theory

According to Merfeld (2011), the application of standard statistical hypothesis testing to the detection of a specific event despite the presence of noise is Signal Detection Theory. In other words, Signal Detection Theory is a general statistical approach that helps make decisions about signals with noise. For example in foggy weather, it is difficult to decide how far away an object is from us, we perceive the object to be further away than it actually is. In this case detection theory can be used to get better results with helping standard statistical hypothesis testing to estimate correct response.

Signal Detection Theory is now used widely in cognitive science as a modeling tool and for the analysis of discrimination and the classification data, Neil A. Macmillan (2005). It also has been applied to physiological responses like threshold, especially when thresholds are measured using tasks that require the subject to select one of two alternative answers, like vestibular system responses. In fact vestibular system responses have some unique characteristics (e.g., bidirectional, vestibular bias, linear, etc.) which let us use the Detection Theory in decision making procedures.

In detection, the subject, attempts to distinguish two stimuli, noise (N) and signal plus noise (S + N), see Figure 6.2.

To apply signal detection theory to our data set we need to have stimuli that are either present or absent.The subjects also need to categorize each trial as having the stimulus present or absent, so the trials are sorted into one of four categories, see Table 6.2.

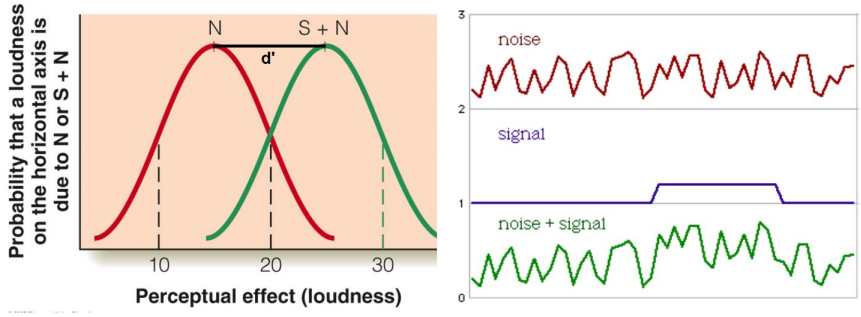

Figure 6.2: Noise and signal plus noise distribution , James (2006)

Table 6.2: Four categories for trials

	Respond "Absent"	Respond "Present"
Stimulus Present	Miss	Hit
Stimulus Absent	Correct Rejection	False Alarm

The subject's ability to detect the stimuli, depends on the overlap between the N and S + N distributions. We call this sensitivity and it is quantified by d', the normalized difference between their means, Figure 6.3 and 6.4.

The goal is to identify each stimulus as an example of N or S + N as accurately as possible. To achieve this we can establish a criterion value of the decision axis and choose one response for points below it, the other for points above it. The placement of the criterion determines both the hits ("yes" responses to signals) and the false alarms ("yes" responses to noise). If the criterion is high (conservative), the subject will make few false alarms, but also not that many hits. By adopting a lower criterion (liberal), the number of hits is increased, but at the expense of also increasing the false alarm rate. The point is this change in the decision strategy does not affect d', Neil A. Macmillan (2005).

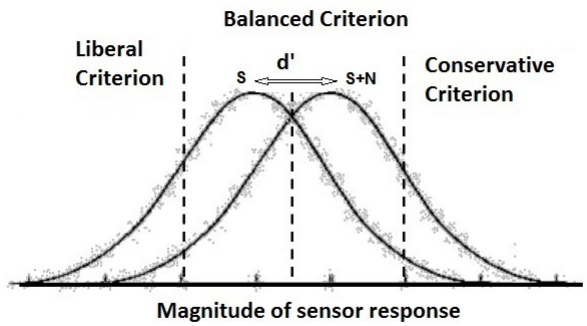

Figure 6.3: The normalized difference between means is sensitivity or d'. Criterion location is strict in (conservative), lax in (liberal), but d' is unchanged, James (2006).

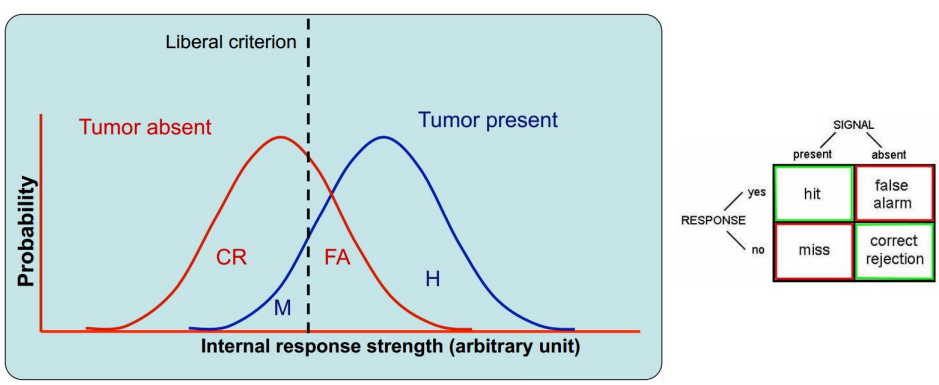

Figure 6.4: Distributions for a Medical tumor diagnosis example. We have CR:Correct rejection FA:False alarm M:Miss H:Hit, James (2006)

Receiver Operating Characteristic (ROC): According to Davis (2006), an ROC curve illustrates the performance of a binary classifier system(true-false or right-left selections) as its discrimination threshold (criterion) is varied. The curve is created by plotting the true positive rate against the false positive rate at various threshold settings. To calculate the statistic of sensitivity (d') we can use an ROC test; however, we always need to assume:

- Underlying distributions in the perceptual space are Gaussian(Normal).
- All distributions have equal variance.

Both of these assumptions need to be used by varying the location of the criterion to construct an ROC curve. In fact the ROC curve is the hit rate as a function of the false-alarm rate, see Figure 6.5.

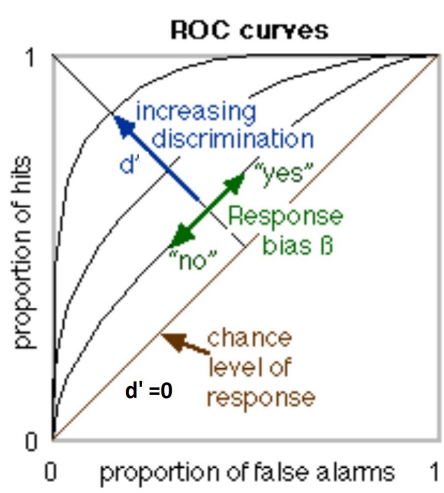

Figure 6.5: An ROC curve, the relation between hit and false-alarm rates, both of which increase as the criterion location moves, Neil A. Macmillan (2005).

We can use an ROC curve to analyze the vestibular system bias and estimate the threshold.

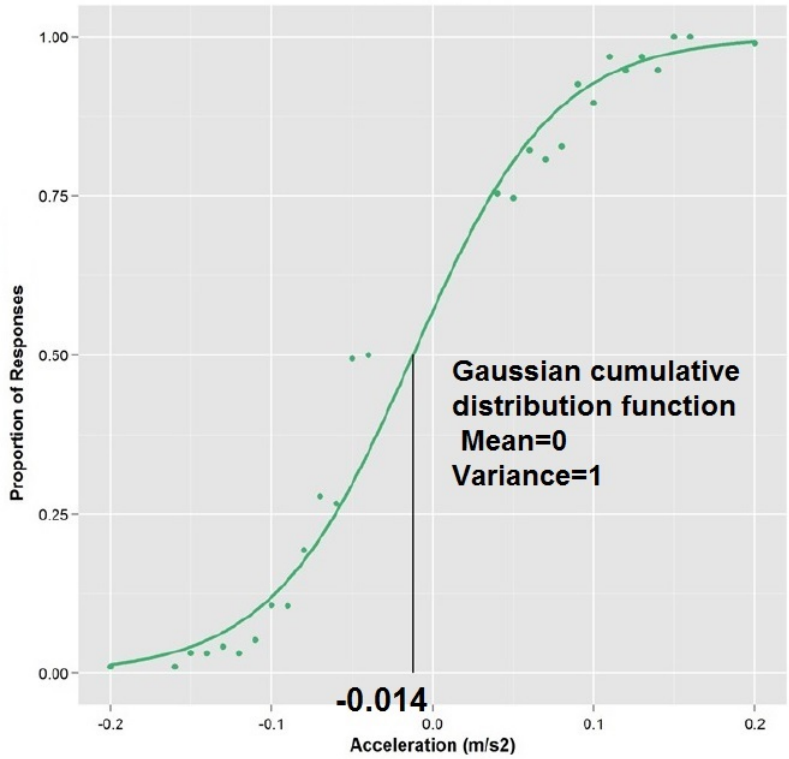

Figure 6.6: Bias in detection of direction of linear motion.

6.2.1 Bias

According to Merfeld (2011) , in psychophysics, a response bias means one response is more probable than another. In other words, a subject may be more likely to respond present or not present for a stimulus. To have correct analysis in response accuracy we always need to consider response bias.

For a detection of motion direction task using bidirectional stimuli, we refer to

bias as the stimulus level that yields the percentage correct midway(50 %) between the lower and upper bounds of the psychometric function, Merfeld (2011). As you can see in Figure 6.6 for forward responses, we can see a negative bias of about -0.014 $\frac{m}{s^2}$ in the backward low acceleration conditions. It means in the presence of null stimuli (zero amplitude acceleration), the subject , on average, experiences stimuli equivalent to $-0.014\frac{m}{s^2}$. In fact there is an unequal contribution from the left and right part of labyrinths in vestibular system which lead to this vestibular bias.

6.2.2 Gaussian Probability density function(PDF):

We know for a given stimulus in a trial that the sensed signal will be randomly selected from a probability distribution(e.g.Gaussian). We also know that a sensed signal closer to the mean is more likely and further away from the mean is less likely. We are using the Probability Density Function (PDF) to describe the likelihood of a sensed signal for this random stimulus. The equation for a Gaussian PDF can be written as shown in Figure 6.7.

6.2.3 Gaussian cumulative distribution functions(CDF):

The cumulative distribution functions (CDF) represent the percentage of times that the participant's perception would be less than or equal the value on the x-axis(e.g. accelerations) for the given mean stimulus. As can be seen in Figure 6.8, the CDF is the integral of the PDF.

We can use the CDF to find vestibular thresholds and bias. This can be read from a graph of the Gaussian cumulative distribution. For example, in Figure 6.6 assume that the criterion is 75%. Using this figure, we can read off the corresponding

acceleration for this criterion. The acceleration shown is about 0.04 m/s^2. It means that in more than 75% of responses the acceleration 0.04 m/s^2 is detected.

6.3 Accuracy improvement analysis

We computed the proportion of correct responses in our four participants through the completion of four sessions, consisting of four blocks within each session(overall 2688 trials). In each block we tested the acceleration profiles in Table 6.3.

According to Figure 6.9, the proportion of correct responses showed that participants correctly identified the direction of stimulus more often when the motion had a larger acceleration relative to when it had a smaller acceleration. Moreover, each participants' task performance improved after four session, 2688 trials (i.e., a learning effect).

As can be seen in Figure 6.9, accuracy improved across sessions mostly for smaller accelerations, whereas there was little to no accuracy improvement across sessions for larger accelerations, which were already close to 100% in the first session.

Table 6.3: Acceleration profiles to do accuracy test

	Acceleration Profiles ($\frac{m}{s^2}$)	Washout ($\frac{m}{s^2}$)
Sessions 1-3	0.2,0.16,0.15,0.14,0.13,0.12,0.11,0.1,0.09,0.08,0.07,0.06,0.05,0.04,-0.04,-0.05,-0.06,-0.07,-0.08,-0.09,-0.1,-0.11,-0.12,-0.13,-0.14,-0.15,-0.16,-0.2	0.01
Session 4	0.15,0.14,0.13,0.12,0.11,0.1,0.09,0.08,0.07,0.06,0.05,0.04,0.03,0.02,-0.02,-0.03,-0.04,-0.05,-0.06,-0.07,-0.08,-0.09,-0.1,-0.11,-0.12,-0.13,-0.14,-0.15	0.01

$$p_X(x) = \frac{1}{\sigma\sqrt{2\pi}} e^{-(x-m)^2/2\sigma^2}$$

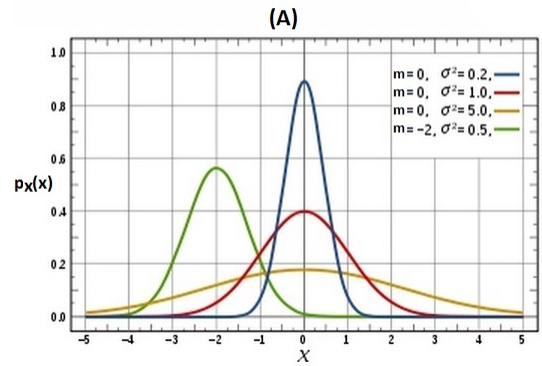

Figure 6.7: Gaussian Probability density function for some mean and variances

$$F_X(x) = \frac{1}{\sigma\sqrt{2\pi}} \int_{-\infty}^{x} e^{-(x-m)^2/2\sigma^2} dx$$

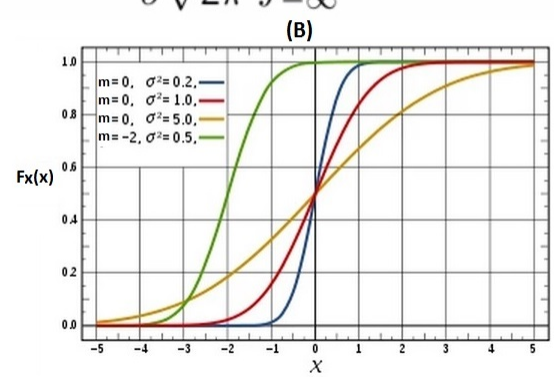

Figure 6.8: Gaussian cumulative distribution function for some means and variances

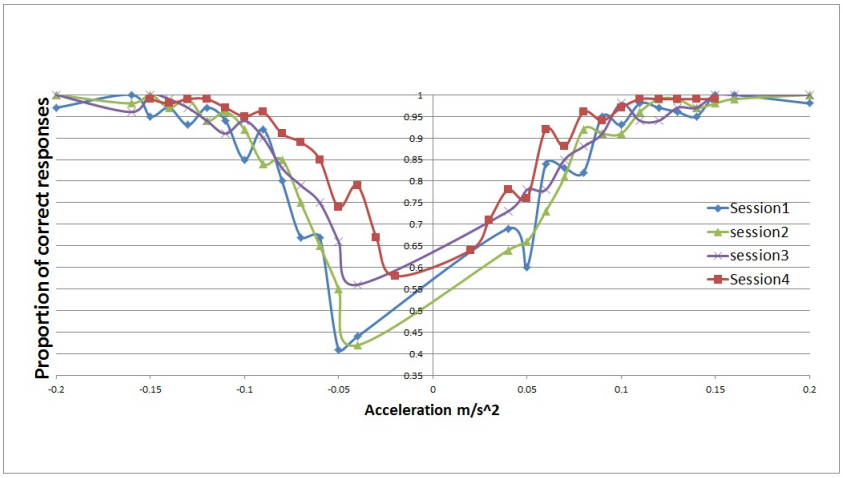

Figure 6.9: We did in overall 2688 trials for each participants. Each point belongs to 96 trials .

6.4 Thresholds analysis

According to Signal Detection Theory, if we consider a Gaussian random variable and a Gaussian distribution for vestibular system thresholds, we can use a probability density function $p_x(x)$ (Figure 6.7) and a Gaussian cumulative distribution function $F_x(x)$ (Figure 6.8) to analyze the collected data and find thresholds.

According to Merfeld (2011), in a direction-recognition task using bidirectional stimuli, as we saw in last part bias is the stimulus level that yields the percentage of detection to 50%, and we used threshold, which is linearly proportional to the standard deviation of the noise is the width of the transition.

After fitting each session's data by Gaussian cumulative distribution function (with Mean=0 and Variance=1)we get the results shown in Figure 6.10. According to this figure, for forward responses the acceleration point associated with 50% forward/backward responses changed from -0.014 in session one to -0.003 in session four.

This acceleration was negative for forward responses, suggesting a small bias in the backward low acceleration conditions.

6.5 Summary of Results

The analysis of the data indicated that in a noisy environment participants could recognize the direction of their movement more accurately when the platform was moved with higher acceleration rather than lower acceleration. In addition, there was a clear training effect across sessions. As the session number increased, the accuracy also increased. Moreover for forward acceleration, we found a negative vestibular bias.

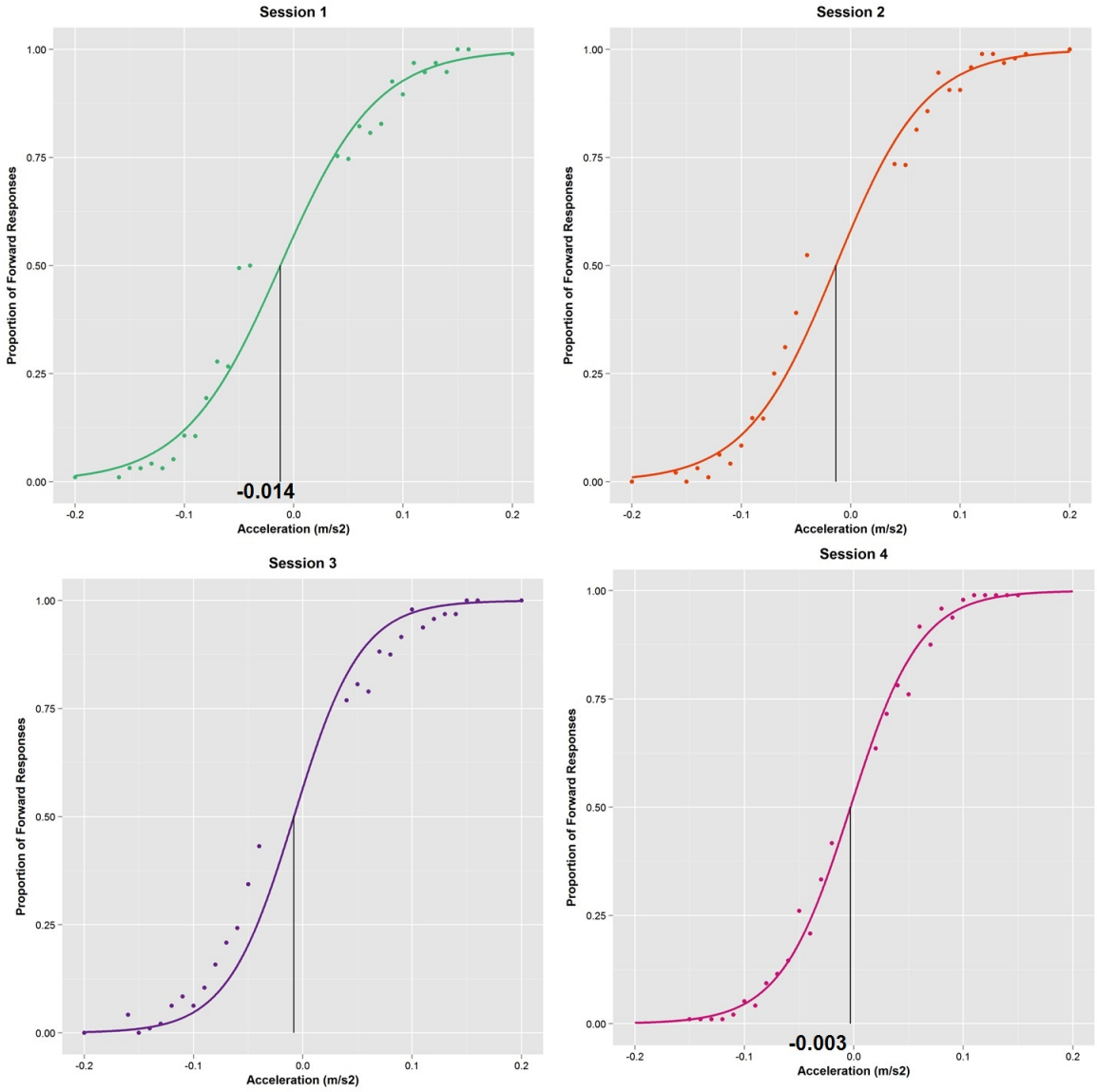

Figure 6.10: Improvement in thresholds after four times test and the backward bias

Chapter 7

Conclusion

We implemented the motion cueing algorithm with vibration and examined the different experiments and analyzed the results. Our results indicated that finding acceleration thresholds is not a simple question to answer. Thresholds depend on many factors and relate to the environment they are presented in. There is also a clear learning process that lasts over the entire experiment of the 4 sessions. There is also a bias in the accelerations where the subject can detect motion but not distinguish direction.

The work was clearly valuable to give us the understanding to design future experiments better.

Possible future works could be investigating the relation between reaction times with the strength of the motion cue. Develop a model for the perception of acceleration by modeling it as a filter. The resulting bandwidth would be a good guide to design motion cueing algorithms.

Bibliography

A.J.Benson, J. and H.Vogel (1986). European vestibular experiments on the spacelab-1 mission: 4. thresholds of perception of whole-body linear oscillation.

Alessandro Beghi, Mattia Bruschetta, F. M. D. M. (2012). A model-based motion cueing strategy for compact driving simulation platforms. *VI-Grade Italy, Via lAquila 1c 33010, Tavagnacco, Udine, Italy.*

Augusto, B. D. C. (2009). Motion cueing in the chalmers driving simulator:an optimization-based control approach.

Bankslap (2009). Vestibular ambiguity http://bankslab.berkeley.edu/projects/projectlinks/pictures

Barnett-Cowan, M. (2013). Vestibular perception is slow a review. *Multisensory research 01/2013; 26(4):387-403. DOI: 10.1163/22134808-00002421.*

Benson, A.J., S. M. B. and Stott, J. R. R. (1986). Thresholds for the detection of the direction of whole-body, linear movement in the horizontal plane. *Aviation, Space, and Environmental Medicine. 57: p. 1088-1096.*

Britannica, E. D. (2009). The physiology of balance: vestibular function.

Chris A. Johnson, B. C. (1999). Properties of staircase procedures for estimating thresholds in automated perimetry .

Colombet, M. Dagdelen, G. R. C. P. F. M. A. K. (2008). Motion cueing: What is the impact on the drivers behavior? *DSC*.

Daniel R. Berger, Jorg Schulte-Pelkum, H. H. B. (2007). Simulating believable forward accelerations on a stewart motion platform.

Davis, Herbert T.; Brown, C. D. (2006). Receiver operating characteristic curves and related decision measures: a tutorial. *Chemometrics and Intelligent Laboratory Systems, 80:24-38*.

Day, B. L. and Fitzpatrick, R. C. (2005). The vestibular system. current biology. *Current Biology Vol.15(No.15):583586.*

DES (2013). Sinusoidal and random vibration testing primer.

Gescheider, G. A. (1997). *Psychophysics: The Fundamentals*. Lawrence Erlbaum Associates ISBN 0-8058-2281-X.

Gianna, Heimbrand S, G. M. (1996). Thresholds for detection of motion direction during passive lateral whole-body acceleration in normal subjects and patients with bilateral loss of labyrinthine function.

G.McConnell, K. (2014). *Vibration Testing, 2nd edition*. Content Technologies, Inc.

Harry J. Zywiol, R. (2003). Motion drive algorithms and simulator design to study motion effects on infantry soldiers.

Hosman, R. (1999). Are criteria for motion cueing and time delays possible? *AIAA-99-4028*.

James, J. D. S. (2006). *Exploring Research Methods in Psychology Using PsychMate*. Psychology Software Tools, Inc.

Jay M. Goldberg, Victor J. Wilson, K. E. C. D. E. A. D. M. B. (2012). *The Vestibular System, A Sixth Sense*. Oxford university press.

Jean-Claude Lepecq, Irini Giannopulu, S. M. and Baudonniere, P.-M. (1999). Vestibular sensitivity and vection chronometry along the spinal axis in erect man. perception. *Perception, 28:6372, 1999*.

Jeremy M. Wolfe, Keith R. Kluender, D. M. L. L. M. B. (2012). *Sensation and Perception, Third Edition*. ISBN-13: 978-0-87893-572-7.

Kathleen Cullen, S. S. (2008). Vestibular system. *McGill university ,Montreal,QC*.

Khaled Fellah, M. G. and Morsly, Y. (2013). Fuzzy/pso basedwashout filter for inertial stimuli restitution in flight simulation.

Kingma, H. (2005). Thresholds for perception of direction of linear acceleration as a possible evaluation of the otolith function.

L.D.Reid, M. (1986). Fligth simulation motion-base drive algorithms: Part 1 developing and testing the equations. technical report. *UTIAS No.296, University of Toronto*.

Mehmet Dagdelen, Gilles Reymond, A. K. M. B. N. M. (2009). Model-based predictive motion cueing strategy for vehicle driving simulators. *ELSEVIER Control Engineering Practice 17(2009) 9951003.*

Merfeld, D. M. (2011). Signal detection theory and vestibular thresholds: I. basic theory and practical considerations. *Experimental Brain Research, 210(3-4), 389405. doi:10.1007/s00221-011-2557-7.*

Moog (2014). Data sheet of electric motion base mb-e-6dof/12/1000kg (formerly 6dof2000e).

Mulder (1908). Quantitative betrekking tusschen prikkel en effect bij het statisehe organ. phd thesis. *University of Utrecht; NASA Technical Translation F-11, 489 (1968).*

Murgovski, N. (2007). Vehicle modelling and washout filter tuning for the chalmers vehicle simulator. *Masters thesis, Chalmers University of Technology, Goteborg - Sweden.*

Neil A. Macmillan, C. D. C. (2005). *Detection Theory: A User's Guide.* Lawrence Erlbaum Associates.

NewPort (2009). Motion control faqs.

Peters, R. A. (1969). Dynamics of the vestibular system and their relation to motion perception, spatial disorientation, and illusions. *NASA CR-1309.*

R.Ercoline, F. H. W. (2004). *Spatial Disorientation in Aviation.* AIAA.

Ross, H. and Murray, D. J. (1996). *E.H.Weber on the tactile senses. 2nd ed.* Hove: Erlbaum (UK) Taylor ,Francis.

Schacter, Daniel L.; Gilbert, D. t. W. D. M. (2010). *Psychology (2nd edition).* MacMillan.

Schroeder, J. A. (1999). Rotorcraft research at the nasa vertical motion simulator. *NASA/TP1999-208766.*

S.Nice, N. (2004). *Control Systems Engineering (Fourth Edition).* John Wiley and Sons,INC.

Strickland, B. B. (2001). *The Gale encyclopedia of psychology.* Gale Group,Psychology.

Telban, R. J. and Cardullo, F. M. (2005). Motion cueing algorithm development: Human-centered linear and nonlinear approaches, technical report. *CR-2005-213747, Nasa.*

Treutwin, B. (1995). Minireview adaptive psychophysical procedures.

v. Mohrenschildt, D. M. (2010). The motion platform and cabin.

Wang, L. (2009). *Model Predictive Control System Design and Implementation Using MATLAB.* Springer.

Zacharias, G. (1978). Motion cue models for pilot-vehicle analysis. *1978, AMRLTR-78-2, Department of Defense, Alexandria, VA.*